A Survey of ^{51}V NMR Spectroscopy

Dieter Rehder

Institut für Anorganische und
Angewandte Chemie der Universität
Martin-Luther-King-Platz 6
D 2000 Hamburg 13, FRG

I. INTRODUCTION

Vanadium-51 is a suitable nucleus for NMR experiments using both Fourier transform (FT) and wide-line equipment. Nuclear data are: natural abundance 99.76 %, nuclear spin 7/2, magnetic moment 5.139 (in units of the nuclear magneton), sensitivity relative to ^{1}H 0.382 at constant magnetic field and 5.52 at constant frequency. Line widths of ^{51}V NMR signals in solution vary from <2 Hz (for vanadium compounds of O_h point symmetry) to ca. 3000 Hz (corresponding to relaxation times of ca. 10 to 0.1 ms), but usually cover the range 20-200 Hz, reflecting comparatively small quadrupolar interactions, which allow observation of sufficiently

Table 1. ^{51}V NMR Data of Carbonylvanadium and Related Complexes

Complex[a]	$\delta(^{51}V)$[b] [ppm]	$^{1}J(^{31}P-^{51}V)$ [Hz]	References
$[V(CO)_6]^-$	-1952		26,43
$[V(CO)_5L]^-$			
L = NH_3[c]	-1670		30
PH_3	-1850	170	31
PF_3	-1961	488	26
$P(OR)_3$	-1910 to -1920	355-370	20,26,31-33
$P(NR_2)_3$	-1780 to -1840	210-230	31,33
$P(alkyl)_3$	-1850 to -1890	185-230	20,26,31-33
$P(t\text{-}Bu_3)$	-1738		e
$P(aryl)_3$[d]	-1805 to -1850	190-350	20,31-33
$P(C{\equiv}CPh)_3$	-1780		e
$As(OEt)_3$	-1862		20
$AsEt_3$	-1850		20
$AsPh_3$[d]	-1800		20,32,34
$Sb(OEt)_3$	-1885		20
$SbEt_3$	-1900		20
$SbPh_3$[d]	-1881		33a
$BiEt_3$	-1743		20
psb(P)	-1814	220	34
psb(Sb)	-1861		34
$[\{V(CO)_5\}_2\mu\text{-}L]^{2-}$			
L = P_2Cy_4	-1889	220	35
P_2Me_4	-1867	207	35
P_2Ph_4	-1850	210	35,36
As_2Ph_4	-1745		35
Sb_2Ph_4	-1740		35
t-dpe	-1836	214	37
dppa	-1823	232	37
arphos(P)	-1847	250	38
arphos(As)	-1823		38
dpae	-1824		38
$[V(CO)_5CN]^{2-}$	-1850[f],-1720[c]		12,30
cis-$[V(CO)_4L]^-$			
L = 2 PH_3	-1830	130	31
2 PF_3	-1967	498	26
2 $P(OR)_3$	-1880 to -1910	365	26,31,33
2 $P(alkyl)_3$	-1720 to -1780	195-215	26,31,33
2 PPh_2Me	-1671		39
PCy_3 + $P(OMe)_3$	-1890	193,381	e
dppm	-1590		39,40
$p_2[5]$	-1755 to -1830	225	37,39,40
dppp, dppb	-1700, -1720	190	39,40
p_3, p_4	-1730 to -1830		39-42
arphos, pab	-1738, -1772	220,240	38,39
dpae, aab	-1730, -1754		38,39
dpap	-1651		39

Table 1. Continued

Complex[a]	$\delta(^{51}V)$[b] [ppm]	$^{1}J(^{31}P-^{51}V)$ [Hz]	References
diars	-1750		39
asb	-1785		34,39
dpsp	-1781		e
cis-$[\{V(CO)_4\}_2\mu\text{-}L_2]^{2-}$			
L = P_2Ph_4	-1780	205	35,36
dpae	-1781		38
$[\{V(CO)_4\}_2(AsPh_2)_2]^{2-}$	-1810		35
mer-$[V(CO)_3L]^-$			
L = p_3	-1720		41,42
p_4	-1810		40,42
cp_3[g]	-1729		42
pp_3	-1724		42
p_2p_4	-1734		46
fac-$[V(CO)_3L]$			
L = p_2p_4	-1778	224	46
3 PF_3	-1964	525	12
trans-$[V(CO)_2(PF_3)_4]^-$	-1948	506	12
$[V(PF_3)_6]$	-1946	510	26,43
$[V_2(CO)_8(CN)_4]^{4-}$[f]	-760		30
$Cp_2V_2(CO)_5$	-1666		e
$CpV(CO)_4$	-1534		26
$CpV(CO)_3L$			
L = PH_3	-1380	155	31
PF_3	-1567	427	26,39
$P(OR)_3$	-1450 to -1500	260-330	26,31,39,44,45
$P(NR_2)_3$	-1340 to -1360	200-230	31,39,44
PR_3[i]	-1376 to -1420	150-160	26,31,39,44,45
PR_3[i]	-1250 to -1300	110-160	39
$P(aryl)_3$[d]	-1300 to -1326	130-170	31,39,44,45
$PPhCl_2$	-1390	140	39
$As(OEt)_3$	-1310		20
$AsEt_3$	-1350		20
$AsPh_3$[d]	-1230 to -1260		20,45
$Sb(OEt)_3$	-1310		20
$SbEt_3$	-1460		20
$SbPh_3$	-1429		33a
$BiEt_3$	-1125		20
P_2Me_4	-1381	165	35
P_2Cy_4	-1363	140	35
P_2Ph_4	-1407	157	35,36
As_2Ph_4	-1157		35
psb(P)	-1306		34

Table 1. Continued

Complex[a]	$\delta(^{51}V)$[b] [ppm]	$^{1}J(^{31}P\text{-}^{51}V)$ [Hz]	References
$[CpV(CO)_3CN]^-$	-1440		26
$\{CpV(CO)_3\}_2\mu$-L			
L = MePhP-PPhMe	-1390	165	35
t-dpe	-1362		37
dppa	-1343		37
Sb_2ph_4	-1325		35
trans-$[CpV(CO)_2L]$			
L = 2 PF_3	-1573	446	26
2 $P(OR)_3$	-1210 to -1270	340-370	31,33
2 PMe_3	-990	210	31,33
2 $PPhMe_2$	-903	185	31
cis-$[CpV(CO)_2L]$			
L = 2 PF_3	-1608	430	26
2 $P(alkyl)_3$	-1160 to -1250	160	31,44
2 $PPhMe_2$	-1195		31,33
2 $P(OR)_3$	-1190 to -1390	280-300	31,33
2 $P(NMe_2)_3$	-1340	240	31,33
2 PPh_2Me	-1152	108	39
dppm	-870		39,40
$p_2[5]$	-1110 to -1143		37,39,40
dppb	-1360		39,40
p_3	-1176		26,41
arphos, pab	-995, -1030		38,39
dpae, aab	-937, -921		38,39
dpap	-1260		39
diars	-992		39
dpsp	-1042		e
asb	-1008		34,39
cis-$[\{CpV(CO)_2\}_2\mu$-L]			
L = P_2Me_4	-1325		35
P_2Cy_4	-1076		35
MePhP-PPhMe	-1070		35
t-dpe	-1143		37
dppa	-1281		37
$CpV(CO)_2\eta^2$-dppa	-517		37
CpV(CO)L			
L = p_3[k]	-950		k
3 PF_3	-1568	450	12
$CpV(PF_3)_4$	-1475	448	12
$[CpV(CO)_3H]^-$	-1730		46

Table 1. Continued

Complex[a]	$\delta(^{51}V)$[b] [ppm]	$^{1}J(^{31}P-^{51}V)$ [Hz]	References
$[CpV(CO)_2(H)L]^-$			
L = PF_3	-1691	562	e
$P(OEt)_3$	-1603	458	e
PPh_2Et	-1355		e
$CpV(CO)(NO)_2$	-1294		47,48
$CpV(NO)_2PZ_3^1$	-973 to -1265	400-655	47,48
η^3-$C_3H_5V(CO)_3L$			
L = dppm	-1355		39
dppe	-1492		39
dppp	-1348		39
arphos	-1413		e
diars	-1461		e
η^3-$C_3H_4MeV(CO)_3$dppe	-1391		e
η^3-Crotyl$V(CO)_3$dppe	-1445		e
$HV(CO)_4L$			
L = dppm	-1593		39,49
dppe	-1690		39,49
dppp	-1600		39,49
dppb	-1553		39,49
arphos	-1663		46,49
cp_3	-1608		46
$HV(CO)_3L$			
L = p_3^m	-1640		46
p_4	-1665		46
cp_3	-1528	180	46
pp_3	-1690		46
p_2p_4	-1485		46
trans-$[HV(CO)_2L]$			
L = p_4	-1658		46
p_2p_4	-1500 to -1800		46
cis-$[HV(CO)_2pp_3]$	-1541		46
$\{HV(CO)_4\}_2\mu$-p_4	-1685		46
$V(CO)_3NO(PMe_3)_2$	-1332	74	50
$V(CO)_3NO$(dppe)	-1382		50

a) Abbreviations for ligands: pab = o-$C_6H_4(PPh_2)(AsPh_2)$, psb = o-$C_6H_4(PPh_2)(SbPh_2)$, asb = o-$C_6H_4(AsPh_2)(SbPh_2)$, aab = o-$C_6H_4(AsPh_2)_2$, diars = o-$C_6H_4(AsMe)_2$; p_2[5] = phosphines forming chelate 5-rings such as o-$C_6H_4(PPh)_2$, $Ph_2P(CH_2)_2PPh_2$ and cis-$Ph_2PCH=CHPPh_2$; t-dpe = trans-$Ph_2PC=CPPh_2$, dppa = $Ph_2PC\equiv CPPh_2$, arphos = $AsPh_2(CH_2)_2PPh_2$; $Ph_2E(CH_2)_nEPh_2$: E = P (n = 1: dppm, n = 2: dppe,

n = 3: dppp, n = 4 dppb), E = As (n = 2: dpae, n = 3: dpap), E = Sb (n = 3: dpsp); p_3 = $PhP(CH_2CH_2PPh_2)_2$, cp_3 = $CH_3C(CH_2PPh_2)_3$, p_4 = $[Ph_2PCH_2CH_2PPhCH_2]_2$, pp_3 = $P(CH_2CH_2PPh_2)_3$, p_2p_4 = $(Ph_2PCH_2CH_2)_2PCH_2CH_2P(CH_2CH_2PPh_2)_2$. b) Upfield of $VOCl_3$ (neat or in CD_2Cl_2) 0.1 - 0.2 M in THF or THF/CH_3CN 1:1 at room temperature, if not indicated otherwise. c) At ca. 200°K in liquid ammonia. d) Including oligodentate ligands with EPh_2 groups (E = P, As, Sb). e) Unpublished. f) In CH_3CN. g) Geometry unconfirmed (see reference 42). h) $^2J(^{51}V\text{-}^{19}F) \approx 10.3$ Hz. i) Tolman's cone angle < 140°. j) Tolman's cone angle > 170°. k) This complex was formerly assigned trans-$[CpV(CO)_2p_3]$ (26,41) on the basis of IR data. An X-ray analysis of this complex, however, shows that actually three CO groups are substituted (51). l) Data for a variety of $CpV(NO)_2L$ complexes, where L is a ligand containing a C, N, O or S donor/acceptor function, are also reported in Ref. 48. m) Erroneously characterized as $\{V(CO)_3p_3\}_2$ in reference 41. n) $^1J(^{51}V\text{-}^{31}P) + {}^1J(^{51}V - {}^{14}N)$.

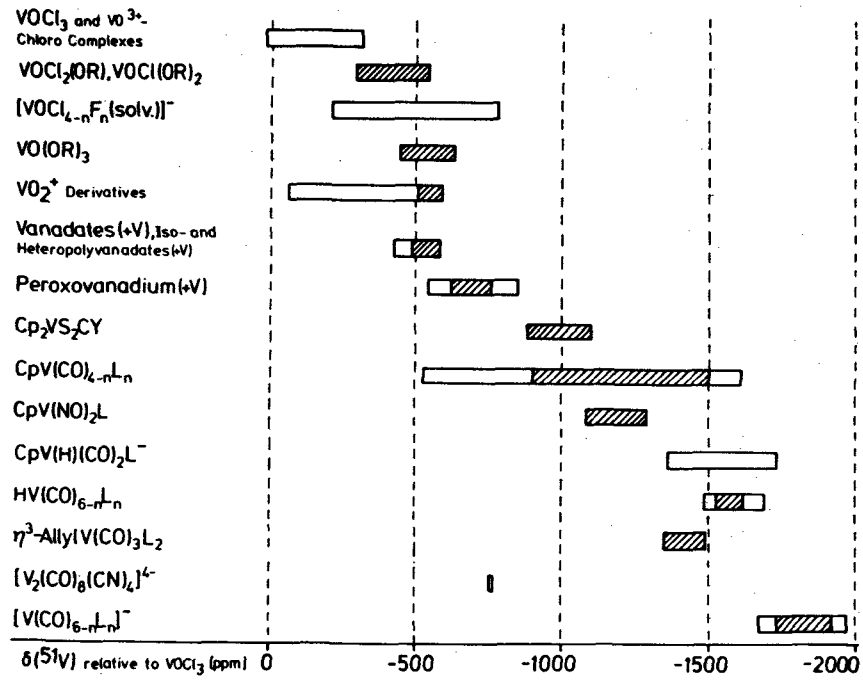

Figure 1. ^{51}V chemical shifts in ppm relative to $VOCl_3$. Not included in this chart is $VOBr_3$ [+ 434 ppm (19)] and current work on sulfido complexes [with low-field shifts down to ca. + 1400 ppm (53)].

onal-pyramidal structure of the $\{V(CO)_{4-n}L_n\}$ moiety. Shielding for these complexes goes down as far as to that of dicyclopentadienyldithioformiatovanadium-(+III) compounds (52) and VOF_3 (19), but does not reach the extremely low shielding values for $VOCl_3$, $VOBr_3$ (19) and sulfidovanadium complexes (down to +1400 ppm (53)). The chart in Figure 1, on first sight, imparts the impression of a correlation between shielding and formal oxidation state. This would imply significant contributions to variations in the overall shielding arising from the local diamagnetic term; we have ruled out this possibility in the previous section. Hence, electronic (and steric) factors have to be taken into consideration to account for these variations.

Qualitative and semi-quantitative MO considerations on $CpV(CO)_3PZ_3$ and $[V(CO)_5PZ_3]^-$ complexes (12,26,32,45) have shown that $\delta(^{51}V)$ values can be used to classify the phosphine ligands PZ_3 according to their ligand strength (σ-donor and π-acceptor ability): the ligand strength increases with increasing negative shift values, i.e. with increasing overall shielding or decreasing paramagnetic deshielding due to enhanced LUMO-HOMO splitting ΔE (equation 7),

$$P(NR_2)_3 \sim P(aryl)_3 < P(alkyl)_3 \sim PH_3 < P(OR)_3 < PF_3$$

This ordering which - except for arylphosphines - is quite similar to the sequence made up on the basis of other (e.g. IR) spectroscopic parameters, also reflects a decrease in metal-contribution to MOs taking part in LUMO-HOMO transitions. The unusual position of PPh_3 (and related phosphines) in this series as compared to its IR-spectroscopic position (where PPh_3 is placed between alkyl- and alkoxyphosphines) has been explained by direct ligand-to-ligand interaction, making PPh_3 a good π-acceptor on the IR but a poor one on the NMR scale (20).

Essentially the same ordering as that for phosphines was established for arsenic and antimony ligands, hence

$$EPh_3 \sim EPh_2CH_2R < EPhMe_2 \sim EEt_3 < E(OEt)_3,$$

where E = P, As, Sb (20,39). This indicates that effects arising from the substituents on E usually override those imparted by the donor/acceptor function of E itself. For an identical set of substituents Z, however (20)

$$BiEt_3 < AsZ_3 < PZ_3 < SbZ_3$$

$$Z_3 = Et_3, Ph_3, Me_2Ph, (OEt)_3$$

and this is paralleled by an analogous ordering of bidentate ligands (38,39):

$$Ph_2As(CH_2)_2AsPh_2 < Ph_2As(CH_2)_2PPh_2 < Ph_2P(CH_2)_2PPh_2$$

and (34,39)

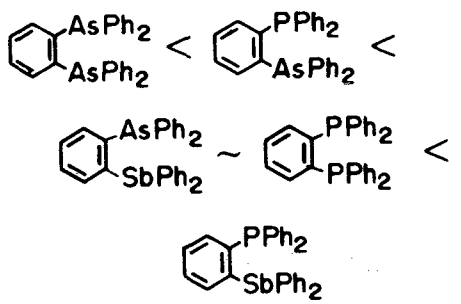

This sequence is independent of the type of complex, which allows an unequivocal assignment of vanadium NMR signals in isomeric mixtures.

While the ordering of phosphorus and arsenic (and bismuth) ligands apparently reflects the order of decreasing ligand strength (decreasing ΔE), the position of antimony ligands such as $SbPh_3$ needs special attention. Here, ΔE appears to be overpowered by the large nephelauxetic effect (small $\langle r^{-3} \rangle_{3d}$) induced by $SbPh_3$, probably connected with an increase in covalency (small k'^2) in going from P to Sb. A similar

conjecture has been made for cobalt complexes (54-56).

The close relationship between the shielding and the ligand strength was also employed to assign signals of vanadium complexes obtained with diphosphanes R_2PPR_2 (35), which form mononuclear, monosubstituted and dinuclear, monosubstituted complexes. The former should exhibit a greater π-interaction due to the presence of an uncoordinated PR_2 group directly bonded to the ligated phosphorus and hence a high $\delta(^{51}V)$ value. This is shown in Figure 2.

Special interest has been focussed on the question of whether PF or CO are the better π-acceptors (12,39,43). The $\delta(^{51}V)$ values for the complexes $CpV(PF_3)_4$ (-1475 ppm) and $[V(PF_3)_6]^-$ (-1946 ppm) are smaller than for the corresponding carbon monoxide compounds ($CpV(CO)_4$: -1534, $[V(CO)_6]^-$: -1952 ppm) and this should suggest a higher π-acceptor power of CO (greater ΔE and smaller paramagnetic deshielding), provided the factor $\langle r^{-3}\rangle_{3d} k'^2$ is constant or overpowered by influences in ΔE. Analogous results are obtained from the ^{93}Nb NMR spectra of octahedral niobium compounds (43). In complexes containing both CO and PF_3 ligands, $\delta(^{51}V)$ are, however, clearly larger for the PF_3 complexes than for the parent carbonyl compounds, although diminished symmetry should increase the number of symmetry-allowed transitions and thus σ_{para}. Figure 3 gives a graphical presentation of the situation. Where PF_3 and CO compete for the metal π-electron density, PF_3 appears to be the better π-acceptor. This statement is valid only with the

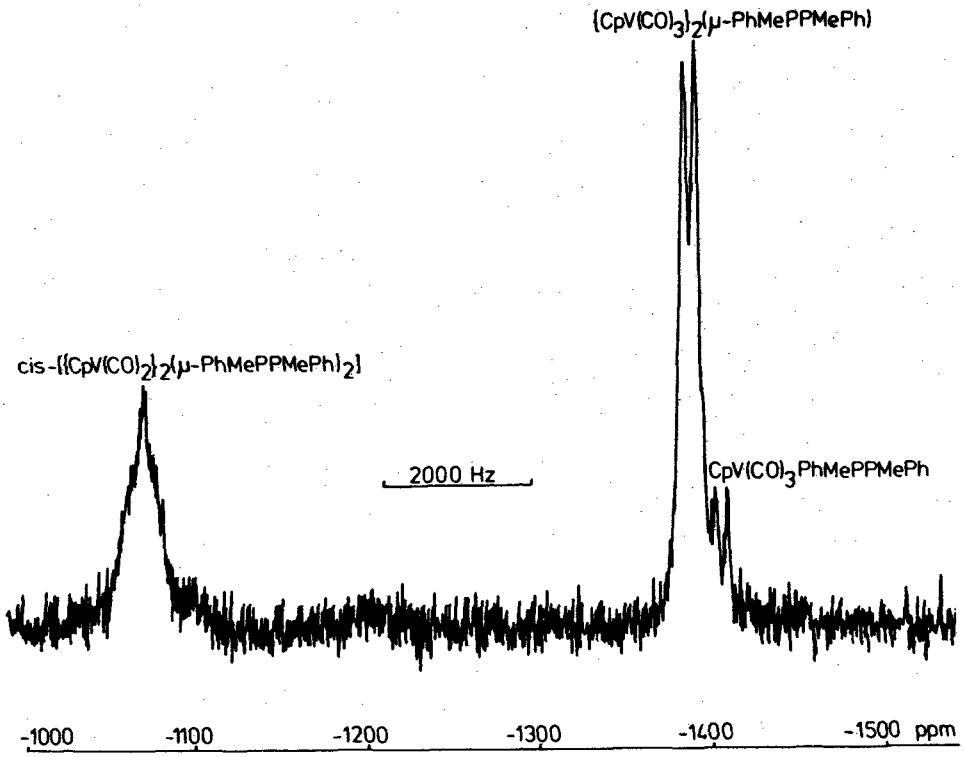

Figure 2. 23.66 MHz ^{51}V NMR spectrum of the reaction products between η^5-$C_5H_5V(CO)_4$ and PhMeP-PMePh.

assumption of constant $\langle r^{-3} \rangle k'^2$ contributions and neglect of anisotropy effects (29).

A symmetry/shielding correlation was also proposed for a number of complexes $[V(CO)_{6-n}(PZ_3)_n]^-$ and $CpV(CO)_{4-n}(PZ_3)_n$ (n = 1 to 3) (26) with the phosphines $P(OMe)_3$, PMe_3, PPh_2Me, and $PhP(CH_2CH_2PPh_2)_2$ (Figure 4), which have substantially lower π-acceptor power than CO or PF_3. Shielding decreases, as CO is successively replaced by the phosphine ligand, which is explained by (i) decreased energy separation between HOMO and LUMO as the degeneracy of the MO taking part in transitions is raised plus increased number of relevant transitions in the complexes of lower symmetry, and (ii) destabilization of σ-type and/or π-type MO as V-PZ_3 interaction becomes increasingly important relative to V-CO interactions. For $[V(CO)_{6-n}(PZ_3)_n]^-$ complexes these relations are shown in Figure 5.

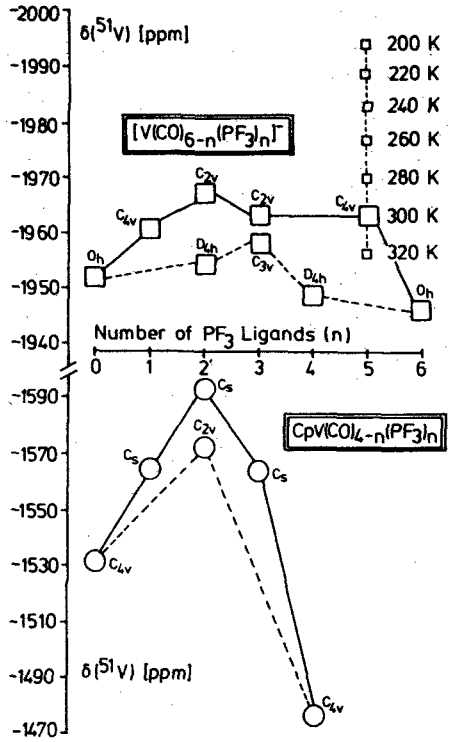

Figure 3. Chemical shifts vs. number of PF_3 ligands in carbonyltrifluorophosphinevanadium complexes, showing the dependence of $\delta(^{51}V)$ upon the local symmetry. Dashed lines connect the higher symmetry isomers. The graph also illustrates the temperature dependence of $\delta(^{51}V)$ for $[Et_4N][V(CO)(PF_3)_5]$(small squares).

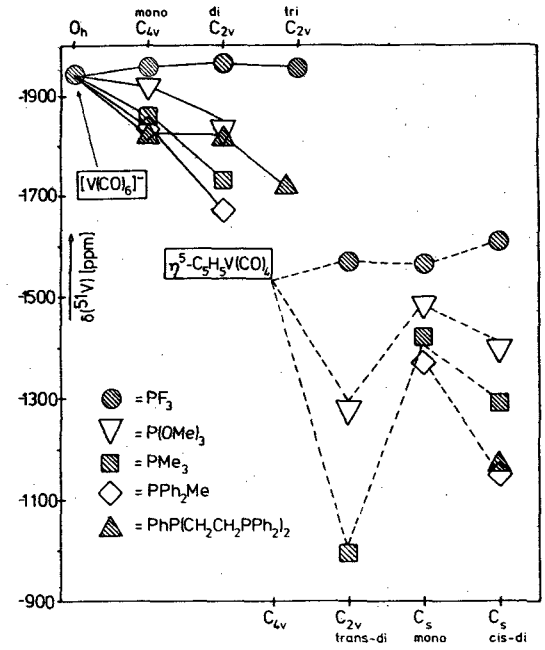

Figure 4. Correlation between chemical shift, local symmetry, and ligand strength for various phosphine derivatives of η^5-$C_5H_5V(CO)_4$ (dashed lines) and $[V(CO)_6]^-$ (solid lines).

Generally, $\delta(^{51}V)$ decreases in the order

$$\{V(CO)_m\} > \{V(CO)_{m-1}\}EZ_3 > \{V(CO)_{m-2}\}(EZ_3)_2 > \{V(CO)_{m-3}\}(EZ_3)_3,$$

where $\{V(CO)_m\} = [V(CO)_6]^-$ or $CpV(CO)_4$; E = P,As,Sb,

and EZ_3 is a mono-, 1/2 di- or 1/3 tridentate ligand. Further, cis-$[V(CO)_{m-2}(PR_3)_2]$ > trans-$[V(CO)_{m-2}(PR_3)_2]$ and fac-$[V(CO)_3(PR_3)_3]$ > mer-$[V(CO)_3(PR_3)_3]$ (R ≠ F).

An additional decrease in ^{51}V shielding is observed with very bulky phosphines. This steric effect is pronounced in the complexes $CpV(NO)_2PR_3$ (47) and $CpV(CO)_3PR_3$ (39) and illustrated for the latter in Figure 6, where Tolman's cone angle is employed as a measure for the ligand size. While variations in $\delta(^{51}V)$ for phosphines of similar cone angles (PF_3, $P(OMe)_3$, $PPhH_2$) again illustrate influences primarily electronic in nature (full circles in Figure 6), the decreasing shielding for alkylphosphines of increasing cone angle (shadowed squares and solid line in Figure 6) is representative for factors primarily steric in nature. The broken line in Figure 6 connects methylphenylphosphines, where either effect has to be taken into account. For bulky phosphines, overlap conditions with suitable vanadium orbitals are less favorable due to steric crowding and increased bond lengths. The validity of the latter argument has been demonstrated by correlating shielding parameters and structural parameters obtained from X-ray analyses of several phosphine-platinum complexes (57-63). The net effect of hindered vanadium-phosphorus interaction is a decrease in ΔE, increase in k'^2 and possibly also an increase in $\langle r^{-3} \rangle$ (diminished extention of the metal-3d system), all of which result in increased paramagnetic deshielding and decreased overall shielding σ. A decrease of shielding due to hindered V-P overlap was also observed in strained chelate-ring structures (39,40) and will be discussed in the context of $\delta(^{31}P)/\delta(^{51}V)$ correlations in Section II. D.

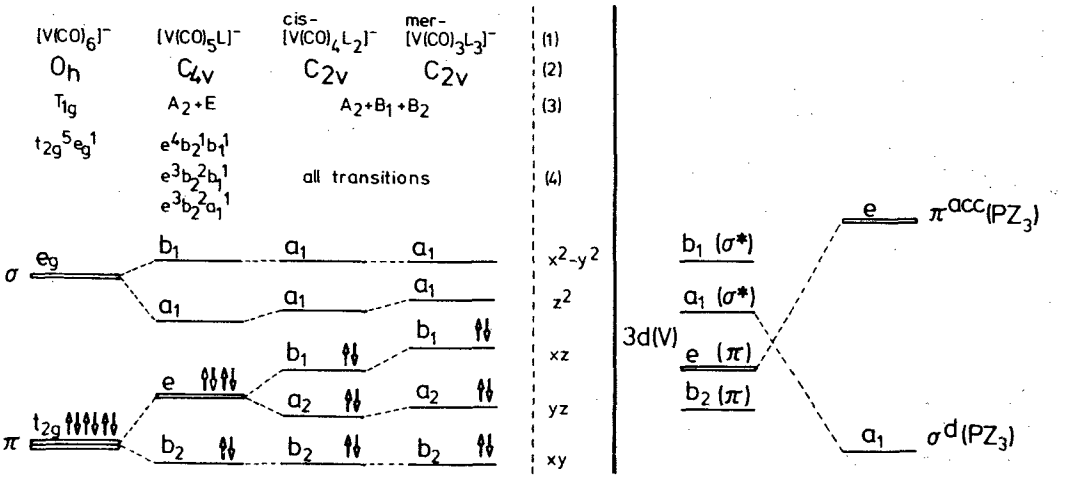

Figure 5. The vanadium-3d system for $[V(CO)_{6-n}L_n]^-$ complexes (left), and the vanadium-phosphorus interaction in $[V(CO)_5PZ_3]^-$ (right). (1) Complex, (2) local symmetry, (3) transformation properties of the angular momentum operator, (4) relevant transitions. From reference (26), slightly revised.

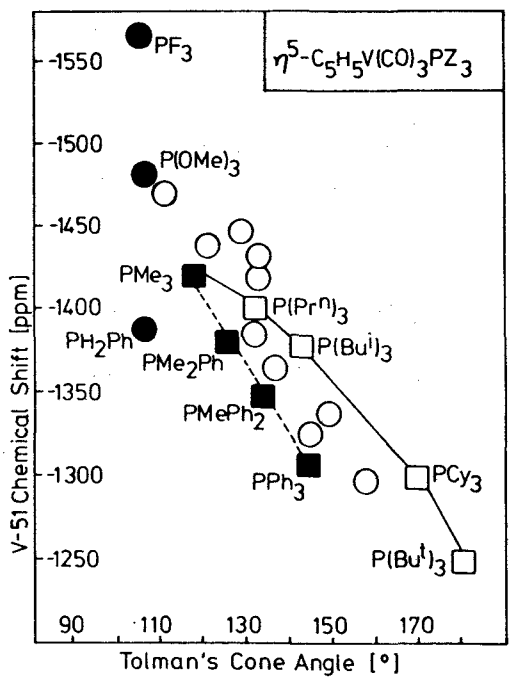

Figure 6. $\delta(^{51}V)$ of η^5-$C_5H_5V(CO)_3PZ_3$ complexes vs. Tolman's cone angles of the phosphines PZ_3. The graph illustrates the dependence of $\delta(^{51}V)$ on steric effects (squares) and electronic effects (full symbols).

2. Thioformiatovanadium(+III) Complexes

^{51}V NMR spectra were obtained for several dicyclopentadienyldithioformiatovanadium-(+III) complexes (Table 2) which, in solution exhibit a temperature dependent equilibrium between a diamagnetic chelate structure with S-S-coordination and an open, paramagnetic form (52):

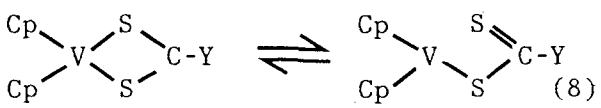

(8)

Since the presence of paramagnetic species usually prevents the observation of vanadium NMR signals, the equilibrium for the compounds listed in Table 2 may be considered to lie, at the temperature indicated, almost exclusively on the side of the diamagnetic forms.

The very similar $\delta(^{51}V)$ values for Y = OEt, NEt_2, PCy_2, PPh_2, and $AsPh_2$ support the assumption that this group does not take part in coordination to vanadium. The same applies to the oxo-phosphorus and thio-phosphorus groups: coordination via the phosphorus-bonded oxygen and sulfur would result in a chelate five-ring structure, for which shielding should be higher than in the four-ring systems (see discussion in Section II. D.). The lower shift values for these complexes are in good agreement with the known weak ligand strength of the ligands $[S_2CP(S)R_2]$ as compared to $[S_2CPR_2]$ (64)

3. Oxovanadium(+V) Complexes Containing the VO^{3+} or VO_2^+ Group

Investigations in this field include compounds of the types VOX_3 (X = F, Cl, Br, NR_2) and $VOCl_{3-n}(OR)_n$ (n = 1-3) (19,65), $[VOF_4]^-$ (66,67) and $[VOCl_{4-n}F_n \cdot CH_3CN]^-$ (n = 0-4) (68), and $[VO_2]^+$ derivatives (69). NMR data are summarized in Table 3.

No $\delta(^{51}V)$ value was reported for

Table 2. ^{51}V NMR Data of Dithioformiatovanadium(+III) Complexes $Cp_2V(S_2CY)$

Y	Solvent	Temperature [°K]	$\delta(^{51}V)$ [ppm]	$\Delta\nu_{1/2}$ * [Hz]
OEt	THF	280	-1100	>3000
NEt_2	THF	300	-1030	
		250	-1080	>3000
PCy_2	CH_2Cl_2	300	-960	
		280	-1000	640
PPh_2	CH_2Cl_2	280	-1040	ca. 1000
$AsPh_2$	CH_2Cl_2	300	-1090	>3000
$P(O)Bz_2$	CH_2Cl_2	250	-895	120
$P(S)Ph_2$	CH_2Cl_2	230	-780	700

*Half-width

Table 3. ^{51}V NMR Data of VO^{3+} and VO_2^+ Complexes

Compound	Phase	$\delta(^{51}V)$ [a] [ppm]	$\Delta\nu_{1/2}$ [Hz]	References
$VOBr_3$	Br_2	+440		19
	neat	+432		19
	CCl_4	+417		19
$[VOCl_4\,CH_3CN]^-$ [b]	CH_3CN	+23		68
$VOCl_3$	neat	0	20	19,2
$VOCl_3(CH_3CN)_2$	THF	-32		19
	CH_3CN [b]	-114	68	
$VOCl_3(PhCN)_2$	THF	-35		19
$VOCl_3/THF$ [c]	THF	-32,-242		
		-316		19
$VO(SClO_3)_3$ [d]	$HSClO_3$	-4		69
$VO(NEt_2)_3$	CH_3CN	-365		19
$VOCl_2OMe$	neat	-290	38	19,e
	THF	-304		19
$VOCl_2OEt$	neat	-300	126	19,e
	THF	-316		19
$VOCl_2(O\text{-}i\text{-}Pr)$	neat	-309	16	19,e
	THF	-342		19
$VOCl_2(O\text{-}n\text{-}Bu)$	neat	-290	63	e
$VOCl_2(O\text{-}i\text{-}Bu)$	neat	-288	28	e
$VOCl_2(O\text{-}t\text{-}Bu)$	neat	-320	19	
	THF	-404	19	
$VOCl(OEt)_2$	neat	-414	770	19,e
$VOCl(O\text{-}i\text{-}Pr)_2$	neat	-506	56	e

Table 3. Continued

Compound	Phase	$\delta(^{51}V)$[a] [ppm]	$\Delta\nu_{1/2}$ [Hz]	References
$VOCl(O\text{-}n\text{-}Bu)_2$	neat	-470	360	e
$VOCl(O\text{-}i\text{-}Bu)_2$	neat	-478	210	e
$VOCl(O\text{-}t\text{-}Bu)_2$	neat	-540	58	e
$VOCl(acac)_2$[f]	THF	-344		19
$V(OMe)_3$	THF	-458		19
	CH_3CN	-459		19
$V(OEt)_3$	neat	-443		19
$VO(O\text{-}n\text{-}Pr)_3$	neat	-555		19
	Et_2O	-584	15	e
	heptane	-577	18	e
	THF	-585	21	e
$VO(Oi\text{-}Pr)_3$	neat	-628	14	19,e
	Et_2O	-624		65
	THF	-619		65
	$C_6H_{11}CH_3$	-623		65
$VO(O\text{-}n\text{-}Bu)_3$	neat	-548		e
	THF	-580	23	19
$VO(O\text{-}i\text{-}Bu)_3$	neat	-538		19
VOF_3	THF	-757		19
	CH_3CN	-786		19
$[VOCl_3F(CH_3CN)]^-$	CH_3CN	-205		68
trans-$[VOCl_2F_2CH_3CN]^-$	CH_3CN	-380		68
cis-$[VOCl_2F_2(CH_3CN)]^-$	CH_3CN	-456		68
$[VOClF_3(CH_3CN)]^-$	CH_3CN	-608		68
$[VOF_4(CH_3CN)]^-$	CH_3CN	-778		68
$[VO(O_2)]^+$	$H_2O/H_2O_2/H^+$	-543	340	70
$[VO_2]^+$	H_2O/H^+	-548	1390-1730	71
	H_2O/pH 0	-545		66
	H_2O/pH 1	-545	850	70,72
	H_2O/pH 2	-541	582	73
$[VO_2(H_2O)_4]^+$	$HClO_4$, HNO_3	-545	400	69
	HCl, H_2SO_4, H_3PO_4	-520 to -587	600-1500	69
$[VO_2(C_2O_4)_2]^{3-}$	H_2O	-533	250	69
$[VO_2(EDTA)]^{3-}$	H_2O	-513	800	69
$[VO_2Cl_2]^-$	CH_3CN	-301	60	69
$[VO_2F_2]^{-g}$	$HSFO_3$	-66	60	69
	DMSO	-64	60	69

a) At room temperature if not indicated otherwise. Some of the shift values reported in reference 19 have been slightly revised. b) At 230°K. c) The three signals probably correspond to $[VOCl_3](THF)_n$, $[VOCl_2(THF)_n]Cl$, and $[VOCl(THF)_n]Cl_2$. d) Tentative assignment for the signal observed when NH_4VO_3 is dissolved in $HSClO_3$. e) Unpublished. f) $acach_2$ = Acetylacetone. g) Tentative assignment.

the $[VOF_4]^-$ anion, the composition of which was based on the observation of a quintet in the vanadium NMR spectrum. Since a quintet is in agreement with the magnetic equivalence of the fluorine ligands established for local C_{4v} symmetry, this geometry was suggested by Hatton et al. (66). According to Moss and Howell (67), however, it is doubtful that the field gradient at the vanadium nucleus is sufficiently small to allow observation of a resolved vanadium signal, and they suggest a rapid exchange amongst the F ligands either in a C_{4v} or in a C_{2v} symmetry or, alternatively, interconversion between these two geometries.

Buslaev and co-workers studied the systems $VOCl_3/CH_3CN$, $VOCl_3/CH_3CN/KCl$, and $VOCl_3/CH_3CN/KF,HF$ (68). For $VOCl_3$ dissolved in CH_3CN, they observed a chemical shift of -114 ppm which they attribute to the known complex $VOCl_3 \cdot 2\,CH_3CN$. The $\delta(^{51}V)$ values reported by us for $VOCl_3 \cdot 2\,CH_3CN$ (-32) and $VOCl_3 \cdot 2$ PhCN (-35 ppm)(19) dissolved in THF may hence correspond to $VOCl_3$/THF adducts (vide infra) formed by displacement of the nitrile for THF. On addition of KCl to a solution of $VOCl_3$ in CH_3CN, a single signal at -38 ppm is obtained which is thought to indicate the position of an exchange equilibrium of the kind

$$VOCl_3 \cdot 2\,CH_3CN + Cl^- \rightleftharpoons [VOCl_4 \cdot CH_3CN]^- + CH_3CN \qquad (9)$$

On lowering the temperature to ca. 230°K, two signals (-114 and +23 ppm) are observed (68).

Rapid exchange among various species also occurs in the $VOCl_3/CH_3CN/HF$ system, for which $\delta(^{51}V)$ values cover the range of -112 to -535 ppm (at room temperature), depending on the $VOCl_3/HF$ ratio. At ca. 240°K, five fluorine-containing complexes can be characterized by distinct ^{51}V NMR signals, where (i) shielding increases with increasing number of F-ligands and (ii) shielding for trans-$[VOCl_2F_2]^-$ is smaller than for the cis-complex. These results are in accord with (i) the stronger ligand field exhibited by the fluoride ligands and (ii) our findings on the shielding in cis/trans isomers of cyclopentadienylcarbonylphosphinevanadium complexes (see Section B. 1.). The relative intensities for a $VOCl_3/HF$ ratio of 1:5 are $[VOCl_4 \cdot CH_3CN]^-$ (0.26) / $[VOCl_3F \cdot CH_3CN]^-$ (0.27) / cis-$[VOCl_2F_2 \cdot CH_3CN]^-$ (0.11) / trans-$[VOCl_2F_2 \cdot CH_3CN]^-$ (0.06)/ $[VOClF_3 \cdot CH_3CN]^-$ (0.16) / $[VOF_4 \cdot CH_3CN]^-$ (0.14). The rapid intermolecular exchange in oxovandium fluorides at room temperature is in contrast to the behaviour of oxofluorochlorides of niobium, for which a ^{93}Nb NMR study has been carried out (74).

The signal at -778 ppm dissolves into a quintet; the corresponding ion $[VOF_4 \cdot CH_3CN]$ apparently is equivalent to that found by Hatton (66) and Howell (67). The shift value reported for VOF_3 dissolved in CH_3CN is -786 ppm (19), which, within the limits of temperature effects, coincides with the $\delta(^{51}V)$ value of $[VOF_4]^-$.

Figure 7 gives a graphical representation of the correlations between the chemical shift values of oxovanadium complexes VOZ_3 and the electronegativity χ of the groups Z, on the one hand, and the bulkiness of R if Z = OR, on the other hand (compare reference 19). Buslaev's data on $[VOCl_{4-n}F_n \cdot CH_3CN]$ have been included (68). There is a consistent upfield trend for the shift values as the electronegativity of Z and the spatial crowding at the VO^{3+} centre increase. The high field shift with increasing χ is consistent with increasing ΔE and decreasing covalency of the V-Z bond (equation 7). The steric influence is opposite to that observed for $CpV(CO)_3PZ_3$ complexes (Figure 6). Lachowicz and Thiele (75,76) have shown that there is a definite tendency for vanadyl esters $VO(OR)_3$ to associate, and this tendency decreases with increasing bulkiness of the alkyl substituent R.

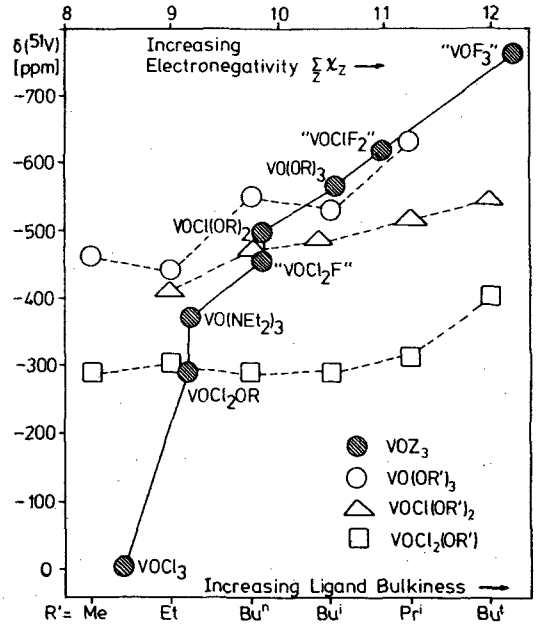

Figure 7. $\delta(^{51}V)$ of VOZ_3 compounds vs. the Allred-Rochow electronegativities χ of the substituents Z (upper abscissa, solid line and shadowed circles; R =n-Bu) and the bulkiness of Z if Z = OR' (lower abscissa, broken lines, and open symbols). Data taken from reference (19) and

We have confirmed this phenomenon by investigating the temperature dependence of the ^{51}V shift values and half widths of the ^{51}V signals. Accordingly, the shifts for the vanadyl esters (and esterchlorides) indicate the equilibrium position of rapid exchange equilibria of the kind

$$n\ VO(OR)_3 \rightleftharpoons \{VO(OR)_3\}_n \qquad (10)$$

where n very likely attains the value 2. At temperatures below ca. 240°K, the two species exhibit two distinct signals (65). If the signal at low field is assigned the oligomeric (dimeric) form, the high field shifts for vanadyl esters containing spacious groups R indicate that there is little association for these compounds (see also the discussion in Section II. E.). An additional contribution to the high field shift may arise from an expansion of the coordination sphere (small $\langle r^{-3} \rangle$ value in equation 7).

Another interesting feature is the substantial upfield shift for $VOBr_3$ and $VOCl_3$ when dissolved in THF (19). The signal for $VOBr_3$ is shifted from +432 to -242 ppm, suggesting a complete rearrangement in the coordination sphere with partial removal of bromine ligands and formation of a species $[VOBr_n(THF)_m]Br_{3-n}$, where n probably = 1. With $VOCl_3$ two signals are obtained. While the low-field signal at -32 ppm may be interpreted in terms of a simple solvent shift (THF coordinated in the second coordination sphere), the high-field signal is probably due to a complex $[VOCl_n(THF)]Cl_{3-n}$, where n varies from 2 ($\delta(^{51}V)$ = -242 ppm for a $VOCl_3$/THF ratio of 1:1) to a limiting value of 1 ($\delta(^{51}V)$ = -316 ppm; $VOCl_3$/THF = 1:10).

Howarth (70) has reported the shift values for the oxovanadium and oxoperoxovanadium cations ($[VO_2]^+$: -545; $[VO(O_2)]^+$: -543 ppm). The shifts are identical within the limits set by the inaccuracy in measuring shift values, but $[VO(O_2)]^+$ is distinct from $[VO_2]^+$ on the grounds of the different line widths and the behaviour towards EDTA: the peroxo compound is not readily chelated by EDTA. The dependence of shift and line width for $[VO_2]^+$ upon concentra-

tion and nature of the acid employed for the acidification of an original metavanadate solution has been discussed by O'Donnell and Pope (69) (cf. Table 3).

4. Vanadates and Peroxovanadates(+V), Iso- and Heteropolyvanadates(+V).

Howarth (70) has also investigated the system metavanadate (i.e. $[H_2VO_4]^-$)/H_2O_2/OH^- and identified up to eleven peroxovanadates from their resonances in the vanadium NMR spectrum. The data are contained in Table 4; four of the species have been tentatively assigned. The composition, i.e. the number of peroxo ligands and the degree of protonation, depends on the number of equivalents of H_2O_2 and base added to $[H_2VO_4]^-$ at a starting pH of 8. The complexes formed with one equivalent of H_2O_2 are $[H_2VO_3(O_2)]^-$ (tentative assignment), $[HVO_3(O_2)]^{2-}$ and, at pH > 10, $[HVO_2(O_2)_2]^{2-}$. This species is the only one present if two equivalents of H_2O_2 plus one equivalent of base are added to metavanadate, while the diprotonated complex $[H_2VO_2(O_2)_2]^-$ is formed without the addition of OH^-. Addition of more than 2 equivalents of H_2O_2 yields $[HVO(O_2)_3]^{2-}$. All protonated forms are deprotonated to $[VO_2(O_2)_2]^{3-}$ and $[VO(O_2)_3]^{3-}$ if the pH exceeds 13. Under extreme conditions (substantial excess of H_2O_2 and OH^-), $[V(O_2)_4]^{3-}$ is obtained.

Shift values increase by ca. 50 ppm or less, if protonation occurs ($[HVO_4]^{2-}$ (-534) → $[H_2VO_4]^-$ (-574)), and increases by ca. 100 ppm for each O_2^{2-} ligand replacing the O^{2-} ligand. These trends are explained by an increase of the energy of the ligand-to-metal charge transfer (increased ΔE in equation 7), in connection with an increase of covalency of the V-O bond (decrease of k').

Four groups (66, 70/72/79, 73,69) have investigated the systems metavanadate/OH^- and metavanadate/H_3O^+. The results can be summarized as follows (see also Figure 8 and compare the data contained in Table 4):

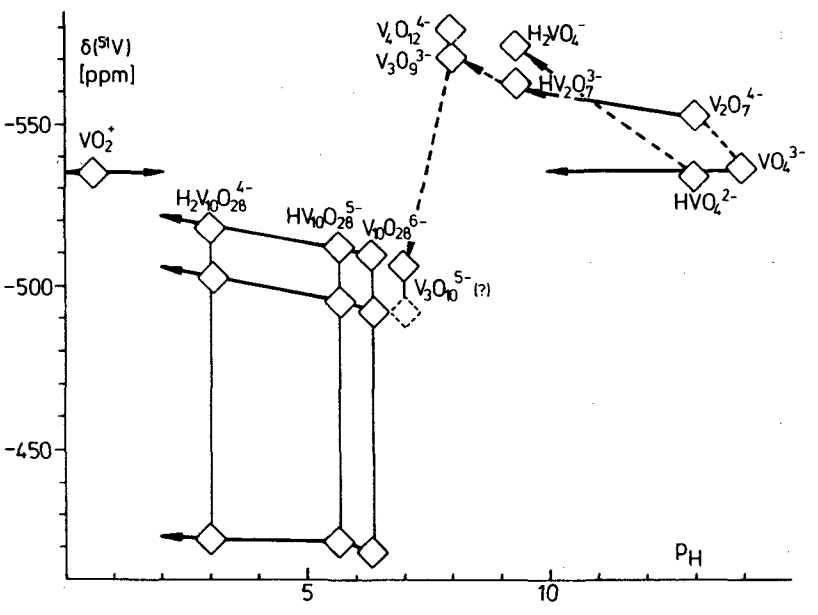

Figure 8. Composition and chemical shifts of vanadates(+V) between pH 0 and 14. Vertical lines connect ^{51}V signals belonging to the same species.

Table 4. ^{51}V NMR Data of Vanadates(+V), Peroxovanadates(+V), and Isopolyvanadates(+V)

Compound	pH	$\delta(^{51}V)$ [ppm] [a]	$\Delta\nu_{1/2}$ [Hz]	References
VO_4^{3-}	14	-536	<10-60	69-73
	>13		27	78
	9	-537	ca 100 [b]	69
	13-10	-554 to -559		66
$VO_3{}^{17}O^{3-}$	>13		50 [c]	78
VO_4H^{2-}	13	-534	50	70,72
$VO_4H_2^-$ ("VO_3^-")	9	-574	80	19,70
$V_2O_7^{4-}$ [b]	13-9	-553 to -568	80-100	69,70
	13-9.5	-527 to -534		66
$V_2O_7H^{3-}$	9	-562		70
$HVO_3(O_2)^{2-}$	10-8	-623	85	70
$H_2VO_3(O_2)^-$ [d]	<8-7	-621		70
$VO_2(O_2)_2{}^{3-}$ [d]	>13	-760	250	70
$HVO_2(O_2)_2{}^{2-}$	13-9	-766	240	70
$H_2VO_2(O_2)_2^-$	5.5	-697	260	70
$H[VO(O_2)_2]_2O^{3-}$	7.5	-757	650	70
$VO(O_2)_3{}^{3-}$	>13	-845	380	70
$HVO(O_2)_3{}^{2-}$	13-5.5	-733	160	70
$V(O_2)_4{}^{3-}$	>13	-734	480	70
$VO(O_2)_2(NH_3)$ [d]	11-7	-746	165	70
$V_3O_{10}{}^{5-}$	6.9-2.7	-493 to -504		
		-510 to -523		66
$V_3O_9{}^{3-}/V_4O_{12}{}^{4-}$ ([d] "$(VO_3)_x{}^{x-}$")	8.5-7.5	-572 to -574	150-180	69
$V_4O_{12}{}^{4-}/V_5O_{14}{}^{3-}$	6.9-2.7	-407 to -419		66
$V_{10}O_{28}6-$	7	-510		
		-492		
		-418		72,79
	5.5	-511		
		-495		
		-426		73
	5-3.5	-510 to -519	150	
		-500 to -504	150	
		-420 to -425	350	69
	4	-520		
		-513		
		-427		73
$HV_{10}O_{28}{}^{5-}$	5.8-4	-512 to -517		
		-495 to -500		
		-421 to -422		79
$H_2V_{10}O_{28}{}^{4-}$	3	-519		
		-502		
		-422		79

a). In aqueous solution at room temperature; resonances cited in reference 70 at 273°K. b) The slightly broader signals and higher shift values at lower pH indicate protonation and exchange equilibria between protonated and unprotonated forms. c) Line width for the V-^{17}O satellites in the ^{51}V NMR spectrum. d) Tentative assignment.

At pH 14, the only species present is the orthovanadate ion $[VO_4]^{3-}$ (-536 ppm) which, due to its tetrahedral geometry (field gradient at the nucleus ≈ 0), is characterized by a narrow line. As the pH is lowered, the signal broadens due to the formation of dimeric $[V_2O_7]^{4-}$ (-553 ppm at pH 13) and protonated species $[HVO_4]^{2-}$ (-534 ppm at pH 13) and $[HV_2O_7]^{3-}$ (-562 ppm at pH 9). Exchange between these species accounts for further line broadening. In the pH region of 8.5 to 7.5, oligomeric metavanadates $[(VO_3)_x]^{x-}$ with x probably 3 and 4 are present (-572 to -576 ppm), but the signal appearing at -574 ppm (pH = 9) is also assigned the diprotonated $[H_2VO_4]^-$ ("metavanadate $[VO_3]^-$"). Further lowering of the pH produces signals which have been associated with the oligomeric anions $[V_3O_{10}]^{5-}$ (two signals at -493 and -510 ppm (pH = 6.9) for the two different vanadium sites in this anion) and tetra- or pentameric forms (ca. -410 ppm) (66). While these are tentative assignments, the existence of decavanadate $[V_{10}O_{28}]^{6-}$ below pH 7 is clearly indicated by a set of three signals [-418 (a), -492 (b), -510 (c) ppm at pH 7 (79)] in the intensity ratio 1:2:2, corresponding to the three different vanadium sites in this anion (Figure 9). Finally, below pH 5.8, the decavanadate is protonated and the species $[HV_{10}O_{28}]^{5-}$ (-421, -496, -512 at pH 5.8) and $[H_2V_{10}O_{28}]^{4-}$ (-422, -501, -519 at pH 3.0) are formed before, in strongly acidic solution (pH < 2), they break down to $[VO_2]^+$ (-545 at pH 0).

Special attention has been attributed to the protonation of $[V_{10}O_{28}]^{6-}$ over the pH range of 9 to 2 (79). The first protonation occurs with an overall pK of ca 5.5, the second protonation at a pK of ca. 3.6. Since the signal (a) is only very slightly affected by the protonation, and since the first protonation affects (c) to a lesser extent than (b) while the influence on (c) and (b) is opposite with the second protonation, the protonation sites are considered to be (b) for the first and (c) for the second protonation (cf. Figure 9). The authors also give strong evidence that the apical out-of-plane, and not the bridging oxygens are protonated,

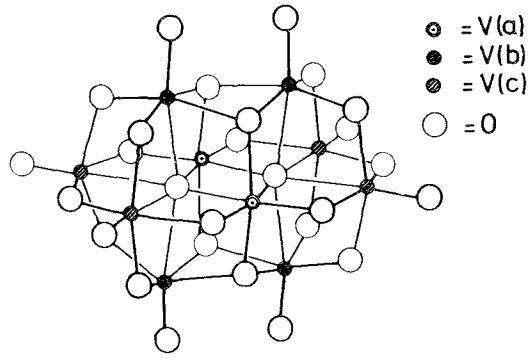

Figure 9. Structure of the decavanadate ion $[V_{10}O_{28}]^{6-}$ [adopted from reference (77)], showing the three different vanadium and the two protonation sites.

which is contrary to the conclusion made on the basis of ^{17}O NMR studies on $[V_{10}O_{28}]^{6-}$ (80).

The ^{51}V NMR spectra of heteropolyvanadates of general formulas $[V_nM_{6-n}O_{19}]^{(n+2)-}$ (n = 1,2), $[V_nM_{13-n}O_{40}]^{(n+2)-}$ (n = 3,4), $[V_nM_{2-n}PO_{40}]^{(n+3)-}$ (n = 1,2) (including some short-living protonated forms), where M = molybdenum and tungsten, have been investigated by four groups (69,71, 73/81, 82), and recently, these studies were extended to $[V_nW_{18-n}P_2O_{62}]^{(n+6)-}$ (n = 1,3) and several heteropolyvanadates containing silicon instead of phosphorus (83). ^{31}P (69,81,82) and ^{17}O NMR studies (82) have also been carried out on selected compounds. ^{51}V data are compiled in Table 5.

Species containing two and more vanadium atoms usually show more than one ^{51}V NMR signal (an exception is $[V_2W_4O_{19}]^{4-}$ (69), which is attributed to isomeric mixtures in solution and/or different vanadium sites in the complex structure. Thus, the lines at -553 ppm for $[V_4W_9O_{40}]^{6-}$ and -558 ppm for $[V_3W_{10}O_{40}]^{5-}$ are allocated to the central (tetrahedral) vanadium in the Keggin structure of these anions, while the lines at ca. -506 and ca. -530 ppm, respectively, are due to external (octahedral) vanadium atoms (69). Heteropolyvanadates - like isopolyvanadates - show a pH-dependent shielding of the ^{51}V nucleus. This is again attributed to protonation, and bridging oxygens are considered to be the protonation sites (69,73,81) which, in the light of the investigations carried out by Howarth and Jarrold on $[V_{10}O_{28}]^{6-}$ (79), seems doubtful.

Chemical shift values are higher for tungsten than for molybdenum anions (compare $[V_2W_4O_{19}]^{4-}$: -513 and $[V_2Mo_4O_{19}]^{4-}$: -502; $[VW_{11}PO_{40}]^{4-}$: -551 and $[VMo_{11}PO_{40}]^{4-}$: -532 ppm (73), and substantially higher for phosphorus-containing heteropolyvanadates. This is rationalized by Kasanskii (73) by considering the first CT transition; i.e. the energy separation between non-bonding orbitals, consisting chiefly of pure p-orbitals localized on the bridging oxygen atoms, and the vacant, basically vanadium-$3d_{xy}$ orbital. The energy of the latter depends on the degree of its participation in the bond between vanadium and suitable bridging oxygens. The Mo-O bond in molybdenum vanadates is weaker than the W-O bond in the tungsten vanadates. Hence, in the former, there is a more substantial participation of oxygen orbitals in the V-O bond and, in turn, a lesser V-d_{xy} contribution. The result is a destabilization of the d_{xy} orbital which leads to higher ΔE and smaller σ_{para} values and thus produces an increase of the overall shielding (equations 7 and 1).

C. Chemical Shifts Related to ESR g-Factors

The ESR-spectroscopic g-factor can be expressed by

$$\Delta g = -2\lambda \sum_n (E_n - E_0) \langle 0|\underline{L}^2|n\rangle \qquad (11)$$

where in the notation of equation 5, λ is the spin-orbit coupling and $\underline{L}$ is the angular momentum operator. Since the vanadium shielding constant depends on the orbital angular momentum and the energy separation between ground state, E_0, and the excited states, E_n, (equation 5), a correlation between $\delta(^{51}V)$ and g values is not unexpected.

An approximately linear correlation has been shown to exist between the $\delta(^{51}V)$ values of the vanadates(+V) $[VW_5O_{19}]^{3-}$, $[VPMo_{11}O_{40}]^{4-}$, $[H_2VW_{11}O_{40}]^{7-}$ and $[VPW_{11}O_{40}]^{4-}$, and the g-factors of the reduced forms with vanadium in the formal oxidation state +IV (73): $|\delta(^{51}V)|$ increases with decreasing g. This correlation was disputed by O'Donnell and Pope (69); it seems to be approximately valid for compounds containing an isolated V atom. Thus, for $[VW_5O_{19}]^{2-}$, $[\alpha VSiW_{11}O_{40}]^{4-}$, $[\alpha_1\text{-}VP_2W_{17}O_{62}]^{6-}$ and $[\alpha_2\text{-}VP_2W_{17}O_{62}]^{6-}$ the respective g-values are 1.962,

reported for phosphorus-containing heteropolyvanadates(+V) (69,81,82) and for carbonylvanadium(-I and +I) complexes (39). In nearly all of the compounds studied, trends in $\delta(^{31}P)$ are opposite to those in $\delta(^{51}V)$, i.e. where shielding of the ^{31}P nucleus decreases throughout a series of comparable complexes, shielding of the ^{51}V nucleus increases. This is demonstrated for selected heteropolyvanadates in Table 6 and for carbonylvanadium complexes in Figure 10.

It is a well established fact that in chelate complexes of the ditertiary phosphines $Ph_2P(CH_2)_nPPh_2$ (diphos; n = 1: dppm, n = 2: dppe, n = 3: dppp, n = 4: dppb), the ^{31}P nucleus is shielded less in the unstrained five-ring than in the strained four-ring structures (84). These relations are paralleled by a contrary trend in the shielding of the metal nucleus (85-87) as exemplified for the ^{51}V nucleus of the complexes $CpV(CO)_2$ diphos and $HV(CO)_4$ diphos in Figure 10. Observations of this kind have been discussed in the light of phosphorus-metal-phosphorus bond angles and metal-phosphorus bond lengths obtained from X-ray data [see 59-63) and literature cited in reference (39)], suggesting that angle distortions (deviations from ideal bond angles) and extended bond lengths in chelate systems subjected to enhanced ring strains cause hindered metal-phosphorus overlap (hence a decrease in ΔE and an increase in metal-d character of the relevant molecular orbitals), and thus decreased overall shielding of the

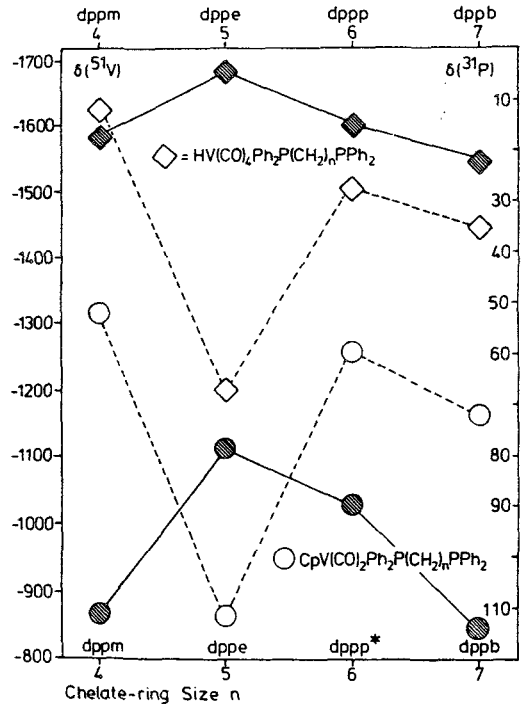

Figure 10. Chelate-ring size vs. $\delta(^{51}V)$(left ordinate, solid lines and shaded symbols) and $\delta(^{31}P)$(right ordinate, broken lines and open symbols). Shielding of the ^{51}V and ^{31}P nuclei increases from bottom to top. The data taken for the dicarbonylcyclopentadienylvanadium 6-ring complex (*) are those of η^5-$C_5H_5V(CO)_2Ph_2(CH_2)_3PPh(CH_2)_3PPh_2$.

metal nucleus in dppm complexes. Simultaneously, bond angles at the phosphorus atom decrease (dppm) or increase (dppp) with respect to the 109° angle for sp^3 hybridization, which is accompanied by an increase of the σ(s) electron density in the donor function and hence an increase in ^{31}P shielding. Hindered P←M π-overlap and a resulting destabilization of the vacant phosphorus type MO taking part in electronic transitions relevant for the paramagnetic shielding of ^{31}P should contribute to the high ^{31}P shielding in the dppm complexes (34,39).

Large ^{51}V upfield shifts for dppe- and large ^{51}V downfield shifts for dppm complexes have also been observed for the complexes cis-$[Et_4N][V(CO)_4$ diphos] and η^3-allyl $V(CO)_3$ diphos (39).

E. Temperature Dependence of ^{51}V Shielding

With increasing temperature, vibronic levels are increasingly populated and thus ΔE in equation 7 will decrease, leading to an increase of the paramagnetic term and a decrease of overall shielding (and $|\delta(^{51}V)$; cf. also references (27) and (88)). This is verified for the phosphomolybdato- and silicotungstatovanadates-(V), where $\delta(^{51}V)$ decreases by 3 to 7 ppm as the temperature is raised from ca. 300° to ca. 350°K (82,83) (cf. Table 5). In carbonylvanadium(+I and -I) complexes, there is usually a linear relationship between $\delta(^{51}V)$ and the temperature in the temperature range 200-340°K (Table 7 and Figure 11; see also Figure 3). Temperature gradients are

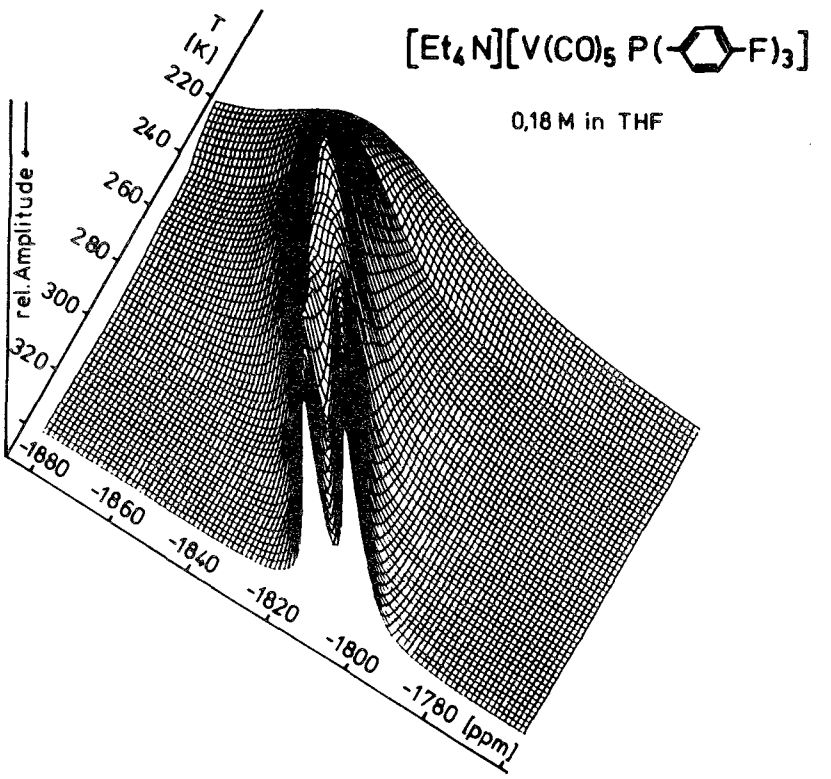

Figure 11. 3D-Plot of $\delta(^{51}V)$ of $[V(CO)_5P(p\text{-}C_6H_4F)_3]^-$ vs. temperature and relative amplitude. The doublet (^{51}V-^{31}P coupling) collapses to a single line below ca. 240°K due to increased line broadening.

around 0.3 ppm/degree for carbonylvanadates(-I) and ca. 0.7 ppm/degree for carbonylvanadium(+I).

In contrast, vanadyltriisopropylate $VO(OiPr)_3$ exhibits a negative temperature gradient; i.e. shielding decreases with decreasing temperature. The temperature dependence of $\delta(^{51}V)$ (and the line-width) of this compound has been subject to an extensive study (65), according to which the decrease of $\delta(^{51}V)$ is the result of increased formation of (probably) dimeric species of lower shielding relative to that of the monomer (equation 10 in Section B. 3.). Below ca. 240°K, the two species emerge as two separate signals (Figure 12 a and b). Over a range of ca. 25 degrees, the signals shift slightly to stronger field, and, starting at ca. 220°K, this trend is again reversed by a second downfield shift which may reflect further aggregation to $\{VO(OiPr)_3\}_n$ ($n > 2$) units.

III. NUCLEAR SPIN-SPIN COUPLING CONSTANTS

A. Introduction and Theory

The main contribution to nuclear spin-spin coupling is usually considered the Fermi contact term (89,90) which, in the average energy approximation, can be written in the form

$$J_{MX} = \frac{32}{9}\pi\gamma_M\gamma_X\beta^2\,\overline{{}^3\Delta E^{-1}}\cdot |S(0)_M|^2|S(0)_X|^2\,\sigma(s)^2 \qquad (13)$$

where $\sigma(s)=2\Sigma c(s)_{iM}\,c(s)_{iX}$. Instead of quoting J, it is sometimes convenient to compare the reduced coupling constants $K = 2\pi J/\hbar\gamma_M\gamma_X$.

$\overline{{}^3\Delta E}$ is the mean triplet excitation energy, $S(0)_M$ and $S(0)_X$ are the respective valence-s wave functions at the nuclei M and X. $\sigma(s)^2$ represents the $\sigma(s)$ contribution to the M-X bond. equation 13 does not contain parameters correlated with direct π-influences. Nonetheless, as we will see, indirect π-contributions are predominant at least in vanadium-phosphorus couplings of carbonylphosphinevanadium complexes. The influence of the $|S(0)_M|^2$ term is demonstrated below for the M-P and M-F couplings of the octahedral complexes $[M(PF_3)_6]^-$ (M = V, Nb). For these complexes, $|S(0)_X|^2$ and - in a first approximation-ΔE^{-1} and $\sigma(s)^2$ may be taken as constant. However, an additional contribution to K(NbP) may arise from the greater σ-bond order in the Nb-P bond.

One of the main problems encountered with couplings in vanadium complexes - as in complexes of other nuclei with nuclear spin > 1/2 - is the quadrupolar line broadening in all complexes but those of cubic and C_{3v} symmetry, which quite often causes unresolved NMR signals. Thus, no coupling constants are reported for phosphorus-containing heteropolyvanadates(+V) (an exception is $[Bu_4N]_3[VW_5O_{19}]$ (83), Table 8), which may, however, also be due to rapid exchange between different isomers or different sites in the same molecule. For the same reason, vanadium-fluorine coupling in complexes such as $[VOF_4]^-$ is only observed at low temperatures (66,67,74).

M	$S(0)^2_{M(-I)}$ (Ref.60)	K_{MP} [Hz]	K_{MF} [Hz] (Ref.43)
V	0.869	154	1.3
Nb	1.788	340	7.7

Table 7. Temperature Dependence of ^{51}V Shift Values

Complex	Phase	Temperature [°K]	$\delta(^{51}V)$ [ppm]	Temp.-Gradient [ppm/°]
$[Na(diglyme)_2][V(CO)_6]$	glyme 0.2 M	340	-1941.5	
		330	-1944.5	
		320	-1947.7	
		310	-1950.9	
		300	-1954.1	
		290	-1957.0	
		280	-1960.2	
		340 - 280		0.313
$[Et_4N][V(CO)_6]$	THF/CH_3CN 1:1, 0.1 M	313	-1951.1	
		303	-1954.2	
		293	-1957.3	
		283	-1960.3	
		273	-1962.9	
		263	-1965.2	
		253	-1967.6	
		243	-1970.2	
		233	-1972.5	
		223	-1974.8	
		203	-1979.1	
		313 - 283		0.32
		283 - 203		0.24
$[Et_4N][V(CO)_5P(p\text{-}C_6H_4F)_3]$	THF 0.2 M	323 - 193	-1805/-1838	0.36
$[Et_4N][V(CO)_5PPhMe_2]$	THF/CH_3CN 1:1, 0.1 M	313 - 213	-1849/-1881	0.32
cis-$[Et_4N][V(CO)_4(PPhMe_2)_2]$	THF/CH_3CN 1:1, 0.1 M	313 - 213	-1702/-1741	0.39
$[Et_4N][V(CO)(PF_3)_5]$	THF 0.1 M	320 - 200	-1957/-1995	0.32
$CpV(CO)_4$	THF	330 - 193	-1514/-1598	0.61
$CpV(CO)_3P(p\text{-}C_6H_4F)_3$	THF 0.2 M	330 - 193	-1300/-1396	0.70
$V_nPW_{12-n}O_{40}^{(n+3)-a}$	H_2O/H_3O^+	345 - 300		0.07 - 0.16

Table 7. Continued

Complex	Phase	Temperature [°K]	$\delta(^{51}V)$ [ppm]	Temp.-Gradient [ppm/°]
α-$K_6HSiV_3W_9O_{40}$ [c]	D_2O/D_3O^+	353 and 303	-566/-571	0.1
β-$K_6HSiV_3W_9O_{40}$ [c]	D_2O/D_3O^+	353 and 303	-569/-575	0.1
$VO(Oi\text{-}Pr)_3$	neat	320 - 240	-627/-623	-0.05
$VO(Oi\text{-}Pr)_3$ [b]	THF 0.86 M	298	-619.7	
		274	-618.1	
		249	-612.0	
		239	-607.2	
		229	-601.6	
		219	-590.9, -601.1	
		209	-581.0, -596.7	
		204	-577.1, -594.8	
		199	-567.8, -590.8	
		195	-563.7, -589.3	
		189	-558.5, -587	
		184	-552.6	
		180	-547.6	
		298 - 180		-0.61 [d]

a) Ref. (82); see also Table 5. b) Ref. (65). c) Ref. (83). d) Averaged for the low field signal. No linear relation.

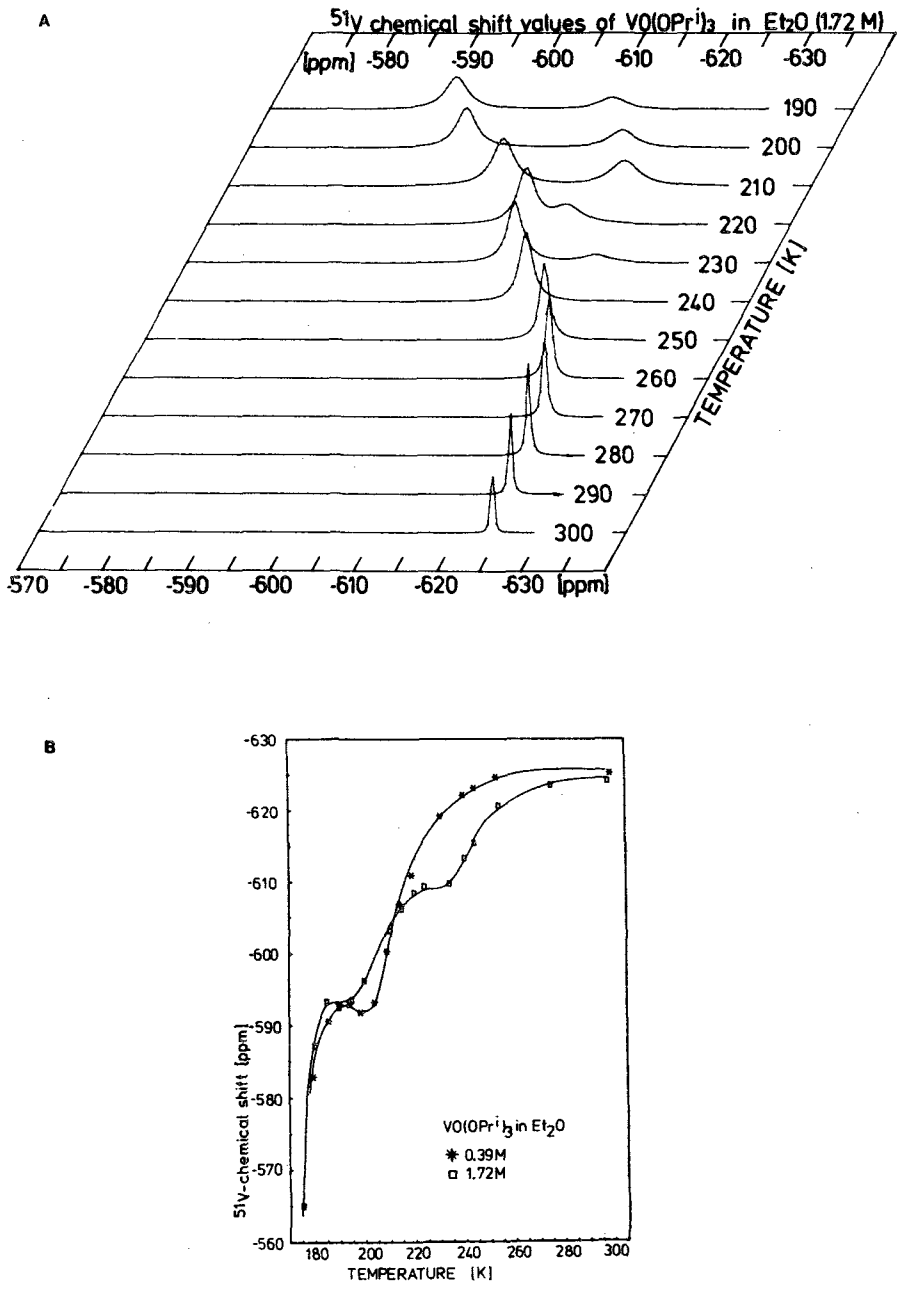

Figure 12. Temperature dependence of ^{51}V shielding in VO(Oi-Pr)$_3$. (a) The signal to low field (T < 240°K) probably corresponds to a dimeric species. Above 240°K, there is rapid exchange between monomeric and dimeric forms. The Figure also shows the line broadening with decreasing temperature. (b) At low concentrations (0.39 M), the inconsistency at ca. 240°K disappears.

On the other hand, vanadium NMR signals in most $[V(CO)_{6-n}(PZ_3)_n]^-$ and $CpV(CO)_{4-n}(PZ_3)_n$ (n = 1,2) complexes are sufficiently narrow so as to allow direct observation of vanadium-phosphorus coupling constants J(VP). This is somewhat surprising, since the local symmetry for these complexes is C_{4v} at the best, and decreases down to C_s in $CpV(CO)_3PZ_3$. In complexes of low point symmetry, the electric nuclear field gradient tensor is fully effective and relaxation times should be rather short. The relatively narrow ^{51}V signals may therefore account for a small electric quadrupole moment eQ of the ^{51}V nucleus as discussed in the introductory section.

The feature of the spectra usually depends on the strength and the bulkiness of the phosphine ligand, the local symmetry of the molecule and the viscosity of the solution. The effect of viscosity is shown in Figure 11: with decreasing temperature, the two lines of the doublet broaden and finally melt to give one broad line. Strong π-accepting ligands give rise to comparatively narrow signals and large coupling constants and thus favor well resolved spectra. In a series of complexes such as $[V(CO)_{6-n}L_n]^-$, line widths increase with decreasing point symmetry, and this dependence sometimes allows for the distinction between geometrical isomers.

A three-fold axis present in the molecule usually decreases the relaxation times to an extent, where coupling is not averaged to zero by rapid quadrupolar relaxation. This is shown in the ^{51}V and ^1H NMR spectra of $[CpV(H)(CO)_3]^-$ (46) (Figure 13). While the vanadium spectrum exhibits a doublet, the eight equidistant signals of equal intensity, which ought to show for the hydride ligand in the ^1H NMR spectrum, overlap to give a plateau-like signal very typical of a spin 1/2 nucleus coupling to a quadrupolar nucleus. An analogous ^1H signal was observed for η^7-$C_7H_7V(CO)_3$ at room temperature (91). The signal successively collapses into a broad Lorentzian line as the temperature is dropped. Finally, in the hydrido complexes $HV(CO)_n p_m$ (n = 2-4; p_m = oligotertiary phosphine), the ^1H and ^{51}V nuclei are decoupled (an exception is $HV(CO)_3MeC(CH_2PPh_2)_3$ which again contains a C_3 axis), and the line pattern observed in the ^1H - NMR spectrum (hydride region) solely

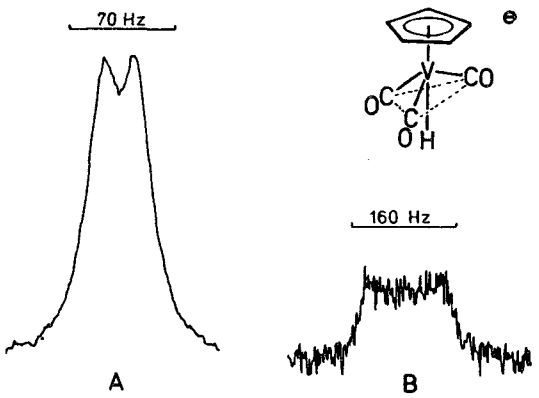

Figure 13. The 23.66 MHz ^{51}V (A) and 270 MHz ^1H (B) NMR spectra of $[Et_4N][\eta^5$-$C_5H_5V(H)(CO)_3]$ (C_{3v} point symmetry for the $[V(H)(CO)_3]$ moiety).

arises from ^{1}H - ^{31}P coupling (46).

^{31}P NMR spectra of phosphinevanadium complexes generally exhibit signals indicating no or only partial decoupling, which are therefore hard to observe. Exceptions are cyclopentadienyl, allyl, and (to a certain extent) hydrido complexes, where sufficiently distinct ^{31}P signals can be observed at 220°K (39-42, 46,92,93). In a few special cases $[CpV(CO)PhP(CH_2CH_2PPh_2)_2]$(51) and allyl complexes (92,93) the ^{31}P and ^{51}V nuclei decouple at low temperature, and a single, rather narrow line is seen in the ^{31}P NMR spectrum.

If the symmetry is O_h or T_d, the field gradient at the nucleus is zero, and quadrupolar relaxation becomes ineffective. Thus, for $[V(PF_3)_6]^-$, a well resolved ^{31}P spectrum is observed, showing eight (^{31}P-^{51}V coupling) superimposed 1:3:3:1 quartets (^{31}P-^{19}F coupling) (43). The corresponding ^{51}V spectrum is illustrated in Figure 14. A resolved eight-line pattern is also observed in the ^{17}O NMR spectrum of $[VO_4]^{3-}$ (78) and in the ^{13}C NMR spectrum of $[V(CO)_6]^-$ (94). Aqueous $[NH_4][VF_6]$, however, exhibits broad signals in both the ^{19}F (width ca. 200 Hz) and the ^{51}V (ca. 170 Hz) spectra (95), indicating either rapid exchange of the fluorine sites or non-ideal octahedral symmetry. In acetonitrile solution, and at 250°K, an eight-line pattern is observed for this ion (14).

B. Discussion

Except for vanadium-phosphorus couplings, information on coupling constants involving vanadium is scarce. The known data are compiled in Table 8 (for J(VP) see also Table 1). Two-bond couplings have been reported in three cases only ($^{2}J(VF)$ in $[V(PF_3)_6]^-$: 10.3 Hz; $^{2}J(VP)$ in $[V(CO)_5P_2Me_4]^-$: 40 Hz; $^{2}J(VW)$ in $[VW_5O_{19}]^{3-}$: 11 Hz); they are smaller by about an order of magnitude than the one-bond coupling constants $^{1}J(VF)$ (88 to 140 Hz) and $^{1}J(VP)$ (341 Hz in $[V(CO)_5P_2Me_4]^-$).

$^{1}J(^{51}V$-$^{31}P)$ coupling constants have been extensively studied (31) and the results are similar to those obtained for J(PW), J(PPt) and J(PRh) (89).

Steric factors do not seem to impart significant influences on the size of J(VP), except where extreme conditions are encountered as with the very bulky phosphines PCy_3 and $P(t\text{-}Bu)_3$, or with disubstituted, cis-configurated complexes of compar-

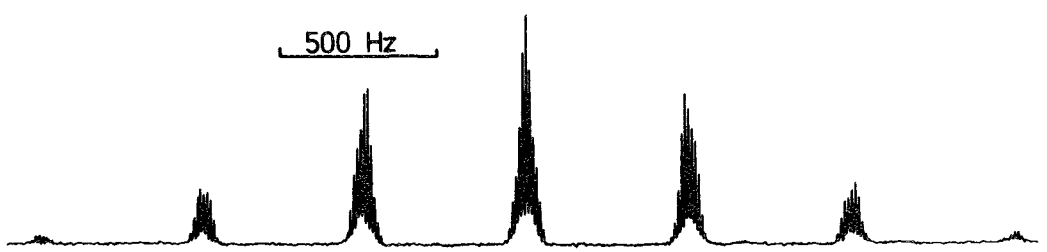

Figure 14. 23.66 MHz ^{51}V NMR spectrum of $[Et_4N][V(PF_3)_6]$, ca. 0.1 M in THF, at room temperature. The fine structure splitting is due to $^{2}J(^{51}V$-$^{19}F)$ coupling.

Table 8. Nuclear Spin-spin Coupling Constants

Complex	Coupling Constant	[Hz]	References
$[CpV(H)(CO)_3]^-$	$^1J(^1H-^{51}V)$	20.3±0.2	46
$[V(CO)_6]^-$	$^1J(^{13}C-^{51}V)$	166	94,96
$(Me_3SiO)_3V{=}Nt\text{-}Bu$	$^1J(^{14}N-^{51}V)$[e]	95	96a
$[VO_4]^{3-}$	$^1J(^{17}O-^{51}V)$	61.6±2.5[a]	78
$[VOF_4]^-$ 263°K	$^1J(^{19}F-^{51}V)$	116±5	66
253°K		120	67
193°K		140	67
$[VF_6]^-$ (MeCN, 253°K)	$^1J(^{19}F-^{51}V)$	88	14
$V(CO)_3(NO)(PMe_3)_2$	$^1J(^{14}N-^{51}V)$/		
	$^1J(^{31}P-^{51}V)$	74[b]	50
$[V(PF_3)_6]^-$	$^1J(^{31}P-^{51}V)$	510	43
	$^2J(^{19}F-^{51}V)$	10.3	43
$[\{V(CO)_5\}_2\mu\text{-}P_2Me_4]^{2-}$	$^1J(^{31}P-^{51}V)$	207	35
$[V(CO)_5P_2Me_4]^-$	$^1J(^{31}P-^{51}V)$	341	35
	$^2J(^{31}P-^{51}V)$	40	c
$cis\text{-}[V(CO)_4PCy_3P(OMe)_3]^-$	$^1J(^{31}PCy-^{51}V)$	193	c
	$^1J(^{31}P(OMe)-^{51}V)$	381	c
$[VW_5O_{19}]^{3-}$	$^2J(^{51}V-^{183}W)$	11	83
$[V(CO)_5PZ_3]^-$	$^1J(^{31}P-^{51}V)$[d]		
$PZ_3 = PF_3$		488	26
$P(OMe)_3$		370	26,31,33
$P(NMe_2)_3$		230	31,33
PMe_3		210	26,31,33
PPh_3		375	c
PH_3		170	31
$cis\text{-}[V(CO)_4(PZ_3)_2]^-$			
$PZ_3 = PF_3$		498	26
$P(OMe)_3$		370	26,31,33
PMe_3		200	26,31,33
PH_3		130	31
$CpV(CO)_3PZ_3$			
$PZ_3 = PF_3$		427	26
$P(OMe)_3$		300	26,31,33
$P(NMe_2)_3$		230	31,33,45
PMe_3		150	26,31,33,45
PCy_3		110	31
$P(t\text{-}Bu)_3$		160	c
PH_3		155	31
PPh_3		157	44
$cis\text{-}[CpV(CO)_2(PZ_3)_2]$			
$PZ_3 = PF_3$		430	26
$P(OMe)_3$		300	26,31,33
$P(NMe_2)_3$		240	31,33
PMe_3		160	26,31,33

Table 8. Continued

Complex	Coupling Constant [Hz]	References
trans-$[CpV(CO)_2(PZ_3)_2]$		
PZ_3 = PF_3	446	26
$P(OMe)_3$	370	26,31
PMe_3	210	26,31
$CpV(NO)_2PZ_3$		
PZ_3 = $P(OMe)_3$	623	48
PMe_3	403	47
$P(t\text{-}Bu)_3$	342	47
PPh_3	403	47

a) Obtained from the ^{17}O NMR spectrum. The coupling constant obtained from the ^{51}V NMR spectrum of ^{17}O enriched VO_4^{3-} is 63 ± 5 Hz. b) Eight-line pattern (relative intensities 1:1.6:2.3:2.5:2.5:2.5:2.3:1.6:1). c) Unpublished or revised. d) Selected data. See also Table 1. e) 1:1:1 Triplet.

atively spacious phosphines ($cis\text{-}[Et_4N][V(CO)_4(PPh_2Me)_2]$ and $cis\text{-}[CpV(CO)_2(PPh_2Me)_2]$ (39)), or with chelate four-ring structures, where hindered σ-overlap may be responsible for a small $\sigma(s)^2$ term in equation 13 and small coupling constants (unresolved spectra).

More pronounced is the dependence of J(VP) upon the type of complex or local symmetry, respectively. Coupling decreases in the order

$$[CpV(H)(CO)_2L] \sim CpV(NO)_2L \gg [V(CO)_5L]^- \gg cis\text{-}[V(CO)_4L_2]^- > CpV(CO)_3L \sim trans\text{-}[CpV(CO)_2L_2] \gg cis\text{-}[CpV(CO)_2L_2]$$

for a given phosphine L such as PMe_3, $P(OMe)_3$, $P(NMe_2)_3$, PH_3 (cf. Table 8). The larger coupling in the pseudo-octahedral anionic complexes relative to that in the square-pyramidal neutral complexes may be due to the higher s-contribution to the hybride orbitals of the former (d^2sp^3) as compared to those of the latter (d^3sp^3) [see, e.g., the discussion of variations in J(RhP) for different hybridization states of rhodium in reference (97)]. The ratio of J(VP) for $[V(CO)_5PZ_3]^-/CpV(CO)_3PZ_3$ varies from 1.1 : 1 to 1.4 : 1. The greater J(VP) values in trans than in $cis\text{-}[CpV(CO)_2(PZ_3)_2]$ parallels an analogous observation for pentacarbonylphosphinetungsten-(0) complexes and was explained by enhanced π-interaction (giving rise to enhanced synergetic σ-donation of the phosphine ligand) in the trans complex (via two orbitals, namely the d_{xz} and d_{yz}) (98). However, a contrary trend ($J_{cis} > J_{trans}$) is observed in most Pt and Rh complexes (89,99,100).

The most obvious alterations in J(VP) originate from electronic factors. J(VP) values correlate with the Allred-Rochow electronegativities $\sum_z \chi_z$ of the substituents Z in the phosphine PZ_3, and similarily with the inductive Taft constants $\sum_z (\sigma_I)_z$ (31). Very bulky phosphines excluded (Tolman's cone angle > 170°), the PZ_3

can be arranged in order of increasing coupling (R = alkyl)

$$PH_3 > PR_3 > P(NR_2)_3 \sim PPh_3 > P(OR)Ph_2 >> P(OR)_2Ph > P(OR)_3 > PF_3$$

The increase of coupling with increased electronegativity of the ligand or the substituents on the donor function of the ligand (see also Figure 15) has been described for a variety of metal-X coupling constants (89, 101-105). From IR data it is well known

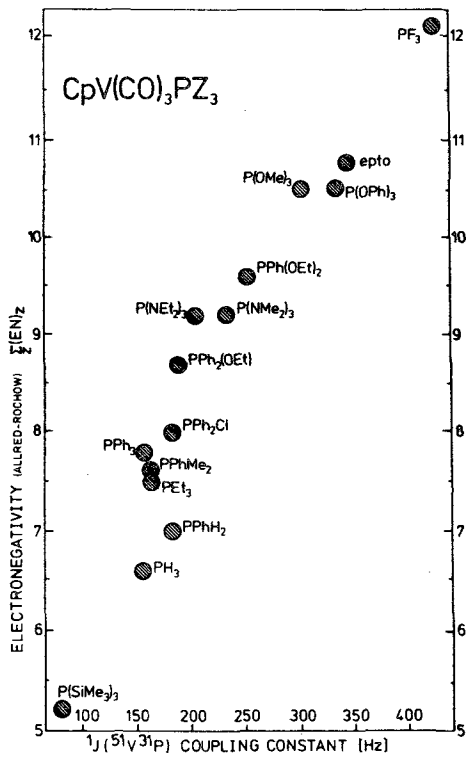

Figure 15. $^1J(^{51}V-^{31}P)$ coupling constants of η^5-$C_5H_5V(CO)_3PZ_3$ complexes vs. the Allred-Rochow electronegativities χ of Z. epto = 4-ethyl-2,6,7-trioxa-1-phosphabicyclo-[2.2.2.]octane.

that increasing electronegativity of Z increases the π-acceptor power of PZ_3. Since the Fermi term (equation 13) does not contain parameters directly connected to π-electron density distributions in the bond under consideration (except, perhaps, for ΔE), interpretation of trends as that shown in Figure 15 has to take into consideration indirect influence of the dominant π-effect on the parameters $|S(0)|^2$ and $\sigma(s)^2$ in equation 13:

(i) Substantial π-delocalization into suitable accepting orbitals located on the phosphine increases the s-contribution to the σ-bonding electron pair on phosphorus via the σ/π synergism, and hence the $\sigma(s)^2$ term.

(ii) V $\rightarrow$ P π-delocalization deshields the ^{51}V nucleus, which results in a contraction of the 4s wave function; i.e. $|S(0)_V|^2$ increases.

(iii) Strongly electronegative Z similarily cause a contraction of the phosphorus 3s wave function and thus increases $|S(0)_P|^2$.

(iv) Electronegative Z should also increase the s-character of the donating electron pair through rehybridization.

The net effects are large coupling constants for phosphines such as PF_3, and $P(OR)_3$, which are usually considered as weak σ-donors, and comparatively small coupling constants for alkylphosphines and PH_3, which are classified as good σ-donors. For aminophosphines, $R_2N \rightarrow P$ p_π-d_π backbonding, as discussed by some workers (106) should be taken into account.

A further influence should arise from ΔE^{-1}, which depends on both, σ- and π-interaction. Strong π-accepting ligands (PF_3, $P(OR)_3$) give rise to large HOMO-LUMO splittings and hence should diminish coupling - contrary to observation. Transitions may therefore be restricted to σ-type molecular orbitals, or effects via ΔE are overridden by the factors mentioned above. This parameter may, however, account for the unexpectedly large coupling encountered with the weak ligands PPh_3 in $[V(CO)_5PR_3]^-$ (375Hz).

C. Correlations between NMR and ESR Coupling Constants ($CpV(CO)_3PZ_3$ and $Fe(NO)_2(PZ_3)Br$)

The relationship between nuclear and electronic spin resonance parameters with special reference to the correlation between NMR coupling constants $^1J(VP)$ of $CpV(CO)_3PZ_3$ and isotropic ESR hyperfine coupling constants $A_{iso}(P)$ of $Fe(NO)_2(PZ_3)Br$ complexes has been reported in reference (44). Correlations of this kind, describing the interacting properties of the phosphine ligands, are not unexpected, since the isotropic ESR hyperfine coupling - like the nuclear spin-spin coupling - is described by a Fermi term

$$A_{iso}(P)=\text{const.}c_s^2(P)|\Psi_0(0)|^2 \qquad (14)$$

where $|\Psi_0(0)|^2 \equiv A_0$ is the s-electron density at the nucleus of the free atom. The coefficients $c_s(P)$ are a measure for the $\sigma(s)(PZ_3)$ contribution to the ground state. They depend on the σ-donor strength and - directly via a stabilization of the HOMO, or synergetically - on the π-acceptor strength of PZ_3 (107).

If the bonding and antibonding σ-type MO for the M-P σ-interaction (M = V, Fe) are Ψ_σ and Ψ_σ^*, respectively, then

$$\Psi_\sigma=\xi\Psi_{M\sigma}+\sqrt{1-\xi^2}\,\Psi_{P\sigma} \qquad (15a)$$

$$\Psi_\sigma^*=\sqrt{1-\xi^2}\,\Psi_{M\sigma}-\xi\Psi_{P\sigma} \qquad (15b)$$

where $\Psi_{P\sigma}=a\psi_{Ps}+\sqrt{1-a^2}\psi_{Pp}$, and $\Psi_{M\sigma}=b\psi_{Ms}+\sqrt{1-b^2}\psi_{Mp}$ Now, equation 13 can be written in the form

$$J(MP)=\text{const.}\bullet|S_P(0)|^2|S_M(0)|^2\cdot$$

$$(^3\Delta E_{\Psi\Psi^*})^{-1}[-a^2b^2\xi^2(1-\xi^2)] \qquad (16)$$

Assuming that changes in M-P σ-bonding (M = Fe, V) impart equal effects on the variables $a^2(1-\xi^2)$ in $CpV(CO)_3PZ_3$ and $C_s^2(P)$ in $Fe(NO)_2(PZ_3)Br$, i.e. assuming $a(1-\xi^2)^{\frac{1}{2}} \propto C_s(P)$, equation (16) becomes

$$J(VP)=\text{const}'.|S_P(0)|^2|S_V(0)|^2$$

$$\overline{^3\Delta E^{-1}}[c_s^2(\varepsilon^2a^2-c_s^2)b^2/a^2] \qquad (17)$$

ε indicates contributions from other orbitals than those considered above.

Assuming further that $|S(0)_V|^2|S(0)_P|^2\Delta E^{-1}$ and the s-coefficients a and b are approximately constant, one arrives, by combination of equations (14) and (17), to a "joint" equation for J(VP) and $A_{iso}(P)$:

$$J(VP)\propto A_{iso}(A-A_{iso}),$$

$$\text{where } A=\varepsilon^2a^2|\Psi_0(0)|^2 \qquad (18)$$

Equation (18) relates the phosphorus-s-orbital contribution to the molecular orbitals relevant for the coupling. Changes in coupling constants can hence be inferred from changes in a single ground state variable, a. The relation is in rather good agreement with findings on 19 phosphines, for which the experimental relation is

$$J(VP) = 0.82A_{iso}(P) + 2.2\bullet10^{-3}[A_{iso}(P)]^2 \qquad (19)$$

The complexes cis-$[CpV(CO)_2(PZ_3)_2]$ also fit this curve.

IV. LINE WIDTHS IN ISOTROPIC MEDIA

Line widths $\Delta\nu_{1/2}$ of ^{51}V NMR signals for all but the carbonyl complexes are contained in Tables 2 to 5. For selected $\Delta\nu_{1/2}$ values of carbonylvanadium complexes see Table 9. It should be mentioned that the lower limit for an accurate determination of line widths on conventional wide-line spectrometers is ca. 50 Hz at best.

A. Exchange Broadening

Under isotropic conditions, quadrupolar effects are restricted to broadening of the NMR signals by quadrupolar relaxation, which is the main relaxation mechanism in systems with quadrupolar nuclei. A second contribution may arise from the dynamic behavior of a system, originating either from inter- or from intramolecular exchange processes provided the exchange is sufficiently fast to suppress detection of the specific forms taking part in the equilibrium.

In various systems containing vanadates, iso- and heteropolyvanadates, line broadening (plus an upfield shift) is observed on acidification. This has been attributed to protonation (giving rise to an increase of the electric field gradient tensor at the nucleus; vide infra), together with rapid exchange between protonated and non-protonated species. Equilibria of this kind involve the systems $[VO_4]^{3-}/[HVO_4]^{2-}$ (72), $[HVO_4]^{2-}/[V_2O_7]^{4-}$ (72), $[V_2O_7]^{4-}/[HV_2O_7]^{3-}$ (72), $[HVO_4]^{2-}/[HV_2O_7]^{3-}$ (69,70) $[HVO_4]^{2-}/[H_2VO_4]^{-}/[VO_3]^{-}$ (70), $[H_xV_2O_7]^{4-x}/[(VO_3)_x]^{x-}$ (x possibly = 3,4) (69), $[V_{10}O_{28}]^{6-}/[HV_{10}O_{28}]^{5-}/[H_2V_{10}O_{28}]^{4-}$ (69,73,79), $[V_{12}PO_{36}]^{7-}/[H_xV_{12}PO_{36}]^{(7-x)-}$ (73), $[V_{12}PO_{40}]^{15-}/[H_8V_{12}PO_{40}]^{7-}$ (81), $[H_2VW_{11}O_{40}]^{7-}/[H_xVW_{11}P_{40}]^{(7-x)-}$ (71), Internal/external proton exchange was discussed for $[H_2VW_{11}O_{40}]^{7-}$ by O'Donnell (69). To account for the resolved ^{51}V NMR spectrum of $[VOF_4]^-$, Howell and Moss have proposed rapid inter- or intramolecular site exchange of F^- ligands (averaging of the field gradient to a small value) (67).

Exchange broadening contributes to the line widths of the vanadium signals of $VO(OR)_3/[VO(OR)_3]_2$ and $[VO(OR)_3]_2/[VO(OR)_3]_n$ (n > 2) equilibria (compare $VO(OiPr)_3$ in Figure 12). The main contribution, however, arises from quadrupolar broadening.

B. Quadrupolar Broadening

Line widths of nuclei possessing an electric nuclear quadrupole moment (nuclear spin > 1/2) are dominated by a quadrupolar relaxation mechanism which originates from the interaction of the electric nuclear field gradient tensor with unsymmetrical electric fields produced by polar molecules in motion. For the extreme narrowing case ($2\pi\nu_o\tau_c >> 1$, ν_o = NMR frequency, τ_c = molecular correlation time), the relaxation mechanism is described by

$$\Delta\nu_{1/2} \propto \frac{1}{T_1} = \frac{1}{T_2} = \frac{3\pi^2}{10} f(I) \cdot Q'^2 \left(1 + \frac{\eta^2}{3}\right) \tau_c \qquad (20)$$

with $Q' = (e^2 q_{zz} Q)/h$ the electric quadrupole coupling constant (q_{zz} = field gradient in zz-direction, and eQ = quadrupole moment). T_1 and T_2 are the longitudinal and transverse relaxation times, respectively; they are connected with the half-width through $T_2^{-1} = \pi\Delta\nu_{1/2}$, and with the peak-to-peak width of the first derivative of the NMR signal through $T_2^{-1} = \sqrt{3}\pi\Delta\nu_{1/2}$. η is the asymmetry parameter ($\eta = 0$ for axial symmetry), and τ_c correlates with the interaction between solute and solvent molecules; $f(I) = (2I+3)/I^2(2I-1)$ is 0.136 for the ^{51}V nucleus.

From equation 20, it is quite clear that $\Delta\nu_{1/2}$ will increase with decreasing point symmetry (where q becomes more effective; q = 0 for O_h and T_d symmetries) and increasing τ_c (increasing viscosity of the

solution). Further, there should be a sizable electronic effect on q, imparted by the electronic structure in the coordination sphere of the nucleus. Thus, for MAB_5 systems (e.g. $[V(CO)_5PZ_3]^-$), q is related (108) to the metal-to-ligand π- and the ligand-to-metal σ-interaction via

$$q \propto -\pi_B + \pi_A + \tfrac{4}{3}\sigma_B + \tfrac{4}{3}\sigma_A \qquad (21)$$

In Table 9, selected line width data on carbonylvanadium complexes are listed. No quantitative interpretation of the trends can yet be carried out. Qualitatively, the results may be summarized as follows:

(i) A decrease of symmetry ($O_h \rightarrow C_{4v} \rightarrow C_{2v} \rightarrow C_s$; $C_{4v} \rightarrow C_s$) results in a substantial increase in $\Delta\nu_{1/2}$.

(ii) Increase in ligand bulkiness ($PPhMe_2 \rightarrow PPh_3 \rightarrow P(t\text{-}Bu)_3$) increases the solvent-solute interactions and thus $\Delta\nu_{1/2}$.

(iii) Line widths increase as the bonding orbitals of the donor/acceptor function become more diffuse (P → As → Sb).

(iv) Strong π-accepting ligands (PF_3) and σ-donating ligands ($PPhMe_2$) give rise to narrow lines.

(v) Enhanced strains in chelate-ring systems (5-ring → 6-ring → 4-ring) increase $\Delta\nu_{1/2}$.

The relation between the electric field gradient tensor q and the local symmetry at the vanadium nucleus has effectively been employed in the assignment of NMR signals of vanadates(+V) and polyvanadates(+V). O'Donnell and Pope (69) summarize the relations as follows:

Site of symmetry of V	Range of line widths (Hz]
tetrahedral	60 - 100
tetragonal (no neighboring V as in $[VW_5O_{19}]^{3-}$)	60 - 80
tetragonal (with neighboring V as in $[V_{10}O_{28}]^{6-}$)	100-200
rhombic	200-800

Table 9. Selected ^{51}V Line-width Data of Carbonylvanadium Complexes

Complex	Local Symmetry	$\Delta\nu_{1/2}$ [Hz]	$\delta(^{51}V)$ [ppm]
(1) Effect of point symmetry and donor/acceptor function (coordinated atoms underlined)			
(a) $CpV(CO)_4$ derivatives			
$CpV(CO)_4$	C_{4v}	12	-1534
$CpV(CO)_3o\text{-}C_6H_4(\underline{P}Ph_2)_2$	C_s	130	-1312
$CpV(CO)_3o\text{-}C_6H_4(\underline{As}Ph_2)(SbPh_2)$	C_s	245	-1236
$CpV(CO)_3o\text{-}C_6H_4(AsPh_2)(\underline{Sb}Ph_2)$	C_s	320	-1382
$CpV(CO)_2o\text{-}C_6H_4(\underline{As}Ph_2)(\underline{Sb}Ph_2)$	C_s	440	-1008
$CpV(CO)_3o\text{-}C_6H_4(Ph_2P)(\underline{Bi}Ph_2)$	C_s	500	-1260
$cis\text{-}[CpV(CO)_2PhP(CH_2CH_2PPh_2)_2]$	C_s	430	-1176
$CpV(CO)PhP(CH_2CH_2PPh_2)_2$	C_s	620	-970
(b) $[V(CO)_6]^-$ derivatives			
$[V(CO)_6]^-$	O_h	1.4±0.3	-1952
$[V(CO)_5PPh_2Et]^-$	C_{4v}	120	-1842
$cis\text{-}[V(CO)_4(PPh_2Et)_2]^-$	C_{2v}	775	-1685
$mer\text{-}[V(CO)_3PhP(CH_2CH_2PPh_2)_2]^-$	C_{2v}	1900	-1736
$\eta^3\text{-}C_3H_5V(CO)_3Ph_2P(CH_2)_2PPh_2$	C_s	2400	-1492
(2) Effects of point symmetry and ligand strength			
(a) $PPhMe_2$ complexes			
$[V(CO)_5PPhMe_2]^-$	C_{4v}	32	-1855
$cis\text{-}[V(CO)_4(PPhMe_2)_2]^-$	C_{2v}	59	-1710
$CpV(CO)_3PPhMe_2$	C_s	60	-1396
(b) PF_3 complexes			
$[V(CO)_5PF_3]^-$	C_{4v}	40	-1961
$cis\text{-}[V(CO)_4(PF_3)_2]^-$	C_{2v}	48	-1967
$CpV(CO)_3PF_3$	C_s	31	-1565
$cis\text{-}[CpV(CO)_2(PF_3)_2]$	C_s	31	-1608
(3) Effect of ligand bulkiness in $[V(CO)_5PZ_3]^-$ complexes			
PZ_3 = $PPhMe_2$ cone angle 122	C_{4v}	32	-1855
PPh_2Me 132	C_{4v}	160	-1839
PPh_3 145	C_{4v}	136	-1805
PCy_3 170	C_{4v}	89	-1854
$P(t\text{-}Bu)_3$ 182	C_{4v}	420	-1738

Thus, the narrowness of the signals for $[VO_4]^{3-}$ and $[V_2O_7]^{4-}$ is consistent with the symmetrical electrical environment of the vanadium nuclei in these anions. Protonation destroys the high point symmetry, and the signals broaden. On the basis of symmetry considerations, the two comparatively narrow lines (ca. 150 Hz) of $[V_{10}O_{28}]^{6-}$ at ca. -500 and -520 ppm (see Section II. B. 4. and Table 5) can be assigned the "outer-plane" vanadium sites with terminal oxygen (b and c in Figure 9), while the third signal at ca. -420 ppm ($\Delta\nu_{1/2}$ = 350 Hz) corresponds with the "in-plane" (site a in Figure 9) vanadium atoms (69,79). Line widths changes for the three signals on lowering the pH from 7 to 2 were also employed to detect the protonation sites in the decavanadate anion (79).

On the grounds of line-width arguments, the $[VO_2]^+$ (or $[VO_2(H_2O)_4]^+$) ion present at pH values < 2 ($\Delta\nu_{1/2} \approx 400$ Hz) was assigned a cisoid arrangement of the two O^{2-} ligands (69), while the additional broadening (→ 1600 Hz) in HCl, H_2SO_4 and H_3PO_4 may indicate the formation of pseudo-octahedral, cis-configurated (C_{2v}) complexes with the incorporation of chloro and sulfato ligands. In $HSClO_3$ and $HSFO_3$, the signals narrow to 60 Hz, which was tentatively attributed to the formation of the pseudo-tetrahedral anions $[VO_2F_2]^-$ and $[VO_2Cl_2]^-$ (69); the local symmetry remains C_{2v}, though. Likewise, it was argued on the basis of line-width differences between $[VW_5O_{19}]^{3-}$ (34 Hz) and $[V_2W_4O_{19}]^{4-}$ (68 Hz) that the two VO_6 groups in the latter occupy cis-positions in the overall structure (73).

Since the correlation time τ is closely related to the viscosity, line widths increase as the temperature decreases (Figures 11 and 12 a). In O'Reilly's quasi-lattice model (109) relaxation takes place by jump-reorientation into empty sites of a hypothetic lattice. Evaluation of τ in the line of this model (110) leads to

$$\tau_c = \frac{1}{6}\left(\frac{2\pi m}{kT}\right)^{\frac{1}{2}} v_f \exp(E/RT) \quad (22a)$$

where E is the activation energy of rotational reorientation, and v_f is the "free volume" (110). The $\Delta\nu_{1/2}/T$ correlation obtained from equation 22a,

$$\Delta\nu_{1/2} = AT^{-1/2}\exp(B/T) \quad (22b)$$

is in excellent agreement with experimental data for $VO(Oi\text{-}Pr)_3$ dissolved in THF (temperature range 300 - 180 K, $\Delta\nu_{1/2}$ = 10 - 600 Hz; A = 0.39404, B = 1767.56, activation energy for the rotation barrier 14.7 kJ) (65).

Gillen and Noggle (111) investigated the temperature dependence of the relaxation times of the ^{35}Cl and ^{51}V nuclei in neat $VOCl_3$, for which anisotropic reorientation is assumed. From the data (summarized in Table 10), they calculated the Arrhenius activation energies E for the appropriate nuclei and also the rotational diffusion constants for rotation about the C_3 axis ($D_{||}$) and perpendicular to it ($D_\perp$). Recent T_1-studies on neat $VOCl_3$ have confirmed that relaxation in this system is purely quadrupolar (2,10).

V. QUADRUPOLE EFFECTS IN ANISOTROPIC MEDIA

The shape of spectra obtained in anisotropic media (liquid crystals, polycrystalline powders, single crystals) is mainly defined by quadrupole interaction (line broadening, first and second order quadrupole splitting) and anisotropic chemical shift effects. The broadening of lines in solids can additionally be caused by magnetic dipolar coupling. We restrict our attention to effects originating in quadrupolar interactions.

A. Liquid Crystals

In anisotropic mesophases, the NMR signals of quadrupolar nuclei split due to the non-vanishing electric

Table 10. Relaxation Data for Neat $VOCl_3$

^{35}Cl (Ref. 113)		^{51}V (Ref. 113)	
T [°K]	$T_2 \cdot 10^5$ [s]	T [°K]	$T_1 \cdot 10^3$ [s]
339.2	24.2 ± 0.7	298.1	23.2 ± 0.3
316.6	19.4 ± 0.4	279.9	19.2 ± 0.3
297.7	15.3 ± 0.4	255.0	13.8 ± 0.2
273.9	11.5 ± 0.3	234.0	9.72 ± 0.15
255.0	8.53 ± 0.2	217.5	6.89 ± 0.10
234.9	5.81 ± 0.2	199.0	4.42 ± 0.07
214.6	3.87 ± 0.1		
E = 8.91 ± 0.17		E = 8.24 ± 0.25 kJ/Mol	

$$D_{||}(303°K) = 7.0 \cdot 10^{10}\ s^{-1}$$
$$D_{\perp}(303°K) = 4.9 \cdot 10^{10}\ s^{-1}$$

$T_1(^{51}V)$	18 ± 2			ms
$T_1(^{35}Cl)$			0.12	ms
$T_2(^{51}V)$	16	16.3		ms
$T_2(^{35}Cl)$		0.20	0.14	ms
τ_c	15	2.6	$3.2 \cdot 10^{-12}$	s
Ref.	(2)	(150)	(151)	

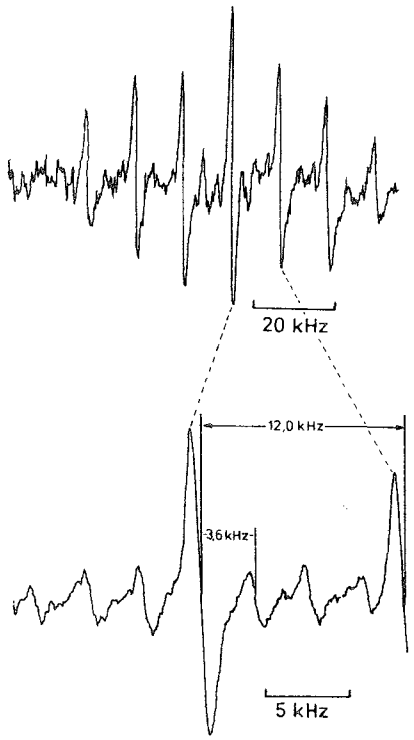

Figure 16. First order quadrupole splitting of the ^{51}V NMR signal (first derivative) of $VO(Oi\text{-}Pr)_3$ dissolved in the liquid crystal MBBA. Two different orderings (anisotropy axes) are shown. The central line corresponds to the $+1/2 \rightarrow -1/2$ transition. Magnetic field = 1 T, frequency = 11.2 MHz.

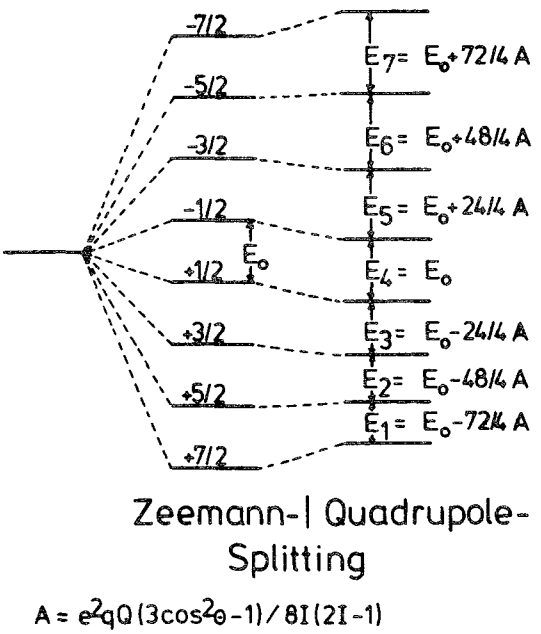

Figure 17. Energy level diagram for the Zeemann splitting in an external magnetic field and first-order quadrupole perturbation for a nucleus of nuclear spin 7/2 (eQ > 0). The scale for the quadrupole splitting is exaggerated by a factor of ca. 10^3. The increase from ΔE_1 to ΔE_2, ΔE_2 to ΔE_3 etc. is 24/4 A, hence the equidistant signals in Figure 16.

field gradient. Accordingly, the ^{51}V NMR signals of vanadyl esters dissolved in liquid crystals show a seven line pattern resulting from a first order quadrupole splitting as shown in Figures 16 and 17, and described by equation 23 (112):

$$E = \gamma\hbar B_o m + \frac{3e^2qQS}{4h(2I-1)} (3\cos^2\theta - 1). [3m^2 - I(I+1)] \quad (23)$$

The first term corresponds to the Zeemann splitting in the external

magnetic field B_o, and the second to the quadrupole splitting. θ is the angle between the director in the liquid crystal and B_o, and S is an ordering factor, denoting the degree of order with respect to a selected molecular axis: $S = 1/2 < 3\cos^2\phi - 1>$ (for cylindrical symmetry), with ϕ the angle between the director and the molecular axis (i.e. the largest component of the field gradient eq). Assuming that $(3\cos^2\phi - 1)$ is averaged to one (113), the quadrupole splitting $\Delta\nu$ between two adjacent lines becomes

$$\Delta\nu = 3e^2qQS/4hI(2I-1) \qquad (24)$$

If S is known, quadrupole coupling constants can be calculated (vide *infra*). Figure 16 illustrates the situation for a solution of vanadyl triisopropylate in the nematic liquid crystal N(p-methoxybenzyliden)p-n-butylaniline (MBBA). The splitting $\Delta\nu$ depends on the concentration and the temperature and is further a function of the mesophase and the vanadyl ester employed (150).

B. Solids

^{51}V NMR results of oxidic vanadium compounds have been reviewed recently by Pletnev (16). We therefore restrict our treatment of this wide area to a compilation of data (Table 11) and a brief mention of several features.

Direct ^{51}V NMR investigations have been carried out on V_2O_5 (115-117), V_nO_{2n-1} (n = 3-8) (118), VO_2 (119-122), $VO_{1.25}$ (123), V_2O_3 (124), vanadium bronzes (125), metavanadates (126-132), divanadates (126,133,134), orthovanadates (126, 135-145), VB (146) and V_3Si (147a), mostly employing polycrystalline powders. However there are also some studies on single crystals (115,116,130,133,134, (141-143) and on amorphous systems (117,131). The phase diagram for $Fe_xNb_xV_{2-2x}O_4$ (x = 0 - 0.09) (121) and V_2O_{3+x} (x = 0 - 0.08) (124) were studied by ^{51}V NMR; and phase transfer in solid solutions was investigated in β-$Na_{0.33}V_2O_5$ (125) and VO_2 containing additives of niobium, chromium and ferric oxide (119; see also Table 11).

A typical ^{51}V NMR spectrum (polycrystalline $VOCl_3$, (150)) is shown in Figure 18. The line pattern originates from first order quadrupole splitting. A similar spectrum was reported for single crystals

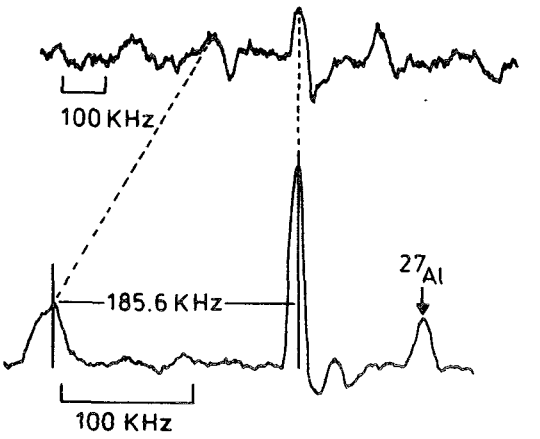

Figure 18. 11.20 MHz ^{51}V NMR spectrum of $VOCl_3$ at ca. 90°K, the lower part showing a section with the split central line and the first satellite (150). Computer simulation for e^2qQ/h = 5.7 MHz indicates an asymmetry parameter η=0.08 (compare the results by Allerhand (149), obtained from the evaluation of the two components of the central line: e^2qQ/h = 5.4 MHz, $\eta \leq 0.4$). The spectrum was obtained on a Varian DP 60 spectrometer at 0.9935 T (sweep width 0.0415 T), with the RF field set to minimal power (10µA on the RF control unit V-4210A). Modulation 0.5 mT; 85 scans.

Table 11. ^{51}V NMR Data of Crystalline Vanadium Compounds[a]

Compound	e^2qQ/h [MHz]	η	σ_1	σ_2	σ_3	σ_{iso}	Refs.
V_2O_5 [b,c]	0.8 ± 0.06						115
V_2O_5 [b,c]	0.805	0.04	2.367	-5.934	3.567		116
VO_2	6.72 ± 0.14	0.51±0.02	-0.33	-0.39	-0.12	-0.28	119,122
$Cr_xNb_xV_{2-2x}O_4$ [d]						-0.28	
(x = 0.01-0.09)	6.72 to 4.76[e]	0.74 to 0.73				to -0.26	119
$Fe_xNb_xV_{2-2x}O_4$ [d]						-0.19	
(x = 0.01-0.09)	6.72 to 4.34[e]	0.50 to 0.79				to -0.27	119
Li_3VO_4 [c]	1.51 ± 0.01		g			-0.1 ± 0.5	135
Na_3VO_4 [c]	1.05 ± 0.03		g			+0.3 ± 0.6	135
$Ca_3(VO_4)_2$ [f]	2.05 ± 0.03		g			+0.1 ± 0.5	135
$Sr_3(VO_4)_2$ [f]	0.53 ± 0.02		g			-0.3 ± 0.5	135
$Ba_3(VO_4)_2$ [f]	0.75 ± 0.02		g			-0.4 ± 0.5	135
$ScVO_4$	3.80 ± 0.04	0	1.0 ± 0.2	1.6	0.8		136
$ScVO_4$						0.96	137
YVO_4	4.75 ± 0.04	0	0.6 ± 0.2	1.6	0.8		136
YVO_4						0.97	137
$LaVO_4$	5.21 ± 0.07	0.69 ± 0.01	i			0.7 ± 0.5	138
$CeVO_4$ [h]	5.23 ± 0.09	0.69 ± 0.03	i			0.5 ± 0.3	138
$CeVO_4$ [h]	5.33 ± 0.07					-1.25	137,144
$PrVO_4$	5.11 ± 0.09	0.76 ± 0.03	i			1.1 ± 0.04	138
$YbVO_4$	4.22 ± 0.04	0	3.5 ± 0.04	5.5	-20.7		136
$CrVO_4$	2.19 ± 0.04					0.31	126
	2.81 ± 0.07[e]						139
$FeVO_4$	2.15 ± 0.04					2.00	126
	1.68 ± 0.14[e]						139
$Co_3(VO_4)_2$	2.16					1.08	126
	2.48 ± 0.08[e]						139
$Ni_3(VO_4)_2$	2.15 ± 0.04					0.76 ± 0.02	126
	2.58 ± 0.01[e]						139
$Ni_2V_2O_7$	3.35 ± 0.06					0.56 ± 0.01	126

Table 11. Continued

Compound	e^2qQ/h [MH]	η	σ_1	σ_2	σ_3	σ_{iso}	Refs.
$Ni(VO_3)_2$	4.03 ± 0.06					0.23 ± 0.01	126
NH_4VO_3	2.88 ± 0.06	0.3 ± 0.10	-1.4 ± 0.2	-0.7	2.7		127
NH_4VO_3	2.76 ± 0.03	0.37 ± 0.05	-1.7 ± 0.2	-0.7	3.0		128
$NaVO_3$	3.65 ± 0.06	0.60 ± 0.10	-1.4 ± 0.2	0.8	3.5		127
$NaVO_3$	3.94 ± 0.04	0.64 ± 0.05	-2.0 ± 0.2	-1.9	3.2		128
$NaVO_3 \cdot 2H_2O$ [j]	4.05 ± 0.05; 2.1	0.22 ± 0.03					129
KVO_3	4.36 ± 0.06	0.75 ± 0.10	-2.3 ± 0.2	-0.3	2.1		127
KVO_3 (glass)	3.35		-1.2	-0.3	3.1		131
KVO_3 [b]	4.22 ± 0.15 [e]	0.65 ± 0.15					130
KVO_3	4.34	0.77	-0.6	-0.9	2.2		132
$CsVO_3$	3.84 ± 0.04 [e]	0.63 ± 0.05	-2.3 ± 0.2	-1.5	3.3		128
$RbVO_3$	4.33 [e]	0.72	-1.4	-1.7	1.7		132
$Mg(VO_3)_2$	6.79 [e]	0.63	-2.4	-2.4	0.9		132
$Ca(VO_3)_2$	2.81 [e]	0.60					132
η^7-$C_7H_7V(CO)_3$ [k]	2.4 ± 0.2	0					148
V_3Si [l]	2.924 ± 0.015	ca 0					147
VOF_3	8.9 ± 0.4	$\leq$ 0.4					149
$VOCl_3$ [m]	5.4 0.2	$\leq$ 0.4					149
$VOCl_3$ [n]	2.98						2
$VOCl_3$ [o]	5.7 ± 0.2	0.08					150
$VOCl_3$ [p]	7.5 ± 0.2						150
$VOCl_2(Oi\text{-}Pr)$ [p]	4.3						150
$VOCl_2(Oi\text{-}Bu)$ [p]	4.7						150
$VOCl_2(OMe)$ [p]	6.0						150
$VOCl(Oi\text{-}Pr)_2$ [p]	7.1						150
$VO(Oi\text{-}Pr)_3$ [q]	4.4 0.3						150
$VO(Oi\text{-}Bu)_3$ [q]	6.4 0.3						150
$VO(On\text{-}Pr)_3$ [q]	5.0 0.4						150

a) See text for explanation of symbols. Standard for the shift values is, if not indicated otherwise, aqueoous KVO_3. Data, except where stated otherwise, at room temperature. b) Single crystal study. c) Standard = Na_3VO_4/aq. d) At 250°K and 315°K, respectively, for details see Ref. 119. e) By multiplication of ν_Q by 14. f) Standard = $Sr_3(VO_4)_2$/aq. g) σ_{aniso} values are as follows: +0.8, -0.9, -0.7, -0.3, -0.4 ± 0.5 h) Data on other MVO_4 (M = Pr, Nd, Sm, Eu, Gd, Tb, Dy, Ho, Er, Tm, Yb, and Lu) are also reported. i) σ_{aniso} =-0.3, -0.3, +0.2; σ_{ax} =-0.5, -0.4, -1.4 in the order $LaVO_3$, $CeVO_3$, $PrVO_3$. j) Two types of non-equivalent vanadium sites. k) Indirectly determined in solution from the ^{51}V spin-lattice relaxation time and from the ^1H line shape, respectively. l) At 28°K. m) At 167°K. n) Determined indirectly from relaxation measurements (cf. text). o) At ca. 90°K. p) Determined from $e^2qQ/h(^{35}Cl)$, $\Delta\nu_{1/2}$ (^{35}Cl-NMR) and $\Delta\nu_{1/2}(^{51}V$ NMR). q) Determined indirectly from quadrupole splittings in nematic liquid crystals.

of V_2O_5 (115), where the splitting of the central line (m = +1/2→m = -1/2) is, however, caused by anisotropic shift interactions. Polycrystalline and amorphous V_2O_5 was investigated by Legrand and co-workers (117). At frequencies >6 MHz, the increase of $\Delta\nu_{1/2}$ with the applied frequency indicates predominance of magnetic interaction (more substantial in crystalline than in amorphous V_2O_5), while at frequencies <6 MHz, the decrease of line widths with the applied frequency both for crystalline and amorphous V_2O_5 indicates predominance of quadrupolar effects. This leads to the assumption of identical local structures at the ^{51}V sites in either species.

An extensive discussion of the theoretical background and analysis of the spectra is given by Baugher et al. (127). The evaluation is carried out according to the following equations (152)

$$\Delta_1 = 3e^2qQ(1-\eta)/2I(2I-1)h \qquad (25)$$

$$\Delta_2 = \frac{25[I(I+1)-3/4](e^2qQ)^2}{64[I(2I-1)]^2h^2\nu_o}\left(1+\frac{74\eta}{135}\cdot\frac{\eta^2}{45}\right) \qquad (26)$$

Δ_1 is the splitting of the central line, Δ_2, the distance between the central line and the first satellite, and ν_o is the generator frequency. It has become common in solid state ^{51}V NMR, to relate the shift values to aqueous KVO_3 ($\delta(^{51}V)$ = -576 ppm upfield of $VOCl_3$) and to quote values in units of 10^{-4} %.

The results for metavanadates show that the tetrahedral symmetry of the basic VO_4 tetrahedron is distorted. It is expected that the primary contribution to the quadrupole coupling constant will be due to substantial π-bonding between vanadium and oxygen. The rather large variations in e^2qQ/h for alkaline metal metavanadates (1.51 - 4.36 MHz) are, however, not easily explained by a π-bond theory. In the sodium metavanadate dihydrate structure, the vanadium atoms are located in two types of nonequivalent sites with different electric field gradients at the vanadium nuclei (129). A ^1H and ^{23}Na NMR study was also carried out on this compound (129). In two papers (132,135) the electric field gradient tensor q has been obtained from semi-empirical Mulliken-Wolfsberg-Helmholtz calculations. The diagonals are

$[VO_3]^-$ (Ref. 132)	$[VO_4]^{3-}$ (Ref. 128)
107.94	-43.164
61.87	80.000
-169.83	123.000

The results for orthovanadates show a similar range of e^2Qq/h values. It was noted that the molecular orbital responsible for the hyperfine interactions at the ^{51}V nucleus is a

$A_1\sigma(s)$ type orbital (139). For two compounds, ESR spectroscopic g-factors are reported: $CrVO_4$, g = 1.98; $FeVO_4$, g = 1.96 (126).

First-order quadrupole splittings of the ^{51}V NMR signals of single crystals of $TmVO_4$ and $GdVO_4$ were observed at temperatures close to absolute zero. For TmVO at 4.5°K, a seven line pattern is obtained which splits into a "double" spectrum at 1.5°K, due to the two principal axes of Jahn-Teller distortion in the (001) plane (141,142). The quadrupole splitting is 160 kHz. A fourteen line system is also observed in $GdVO_4$ (below 2.495°K) which arises from the two different vanadium sites produced by magnetic ordering by Gd^{3+} (143).

Apart from vanadates(+V), information on quadrupole coupling constants for vanadium compounds is scarce (148-150, 2). We have determined e^2qQ/h values for $VOCl_3$ and several vanadyl ester chlorides indirectly through the ^{35}Cl quadrupole coupling constants measured at 77°K, and ^{51}V and ^{35}Cl NMR line widths in the neat samples at room temperature (150). Comparison between e^2qQ/h for $VOCl_3$ obtained by this method (7.5 MHz) and from powder spectra [ca. 5.6 MHz (149,150)] show that the former presumably is too large by approximately 40%. One has, however, to keep in mind that in a frozen liquid such as $VOCl_3$, partial orientation is likely to occur. The e^2qQ/h value of $VOCl_3$ was also estimated from relaxation data [2.98 MHz, (2)], using the Debye-Stokes-Einstein equation for the calculation of τ_c; it seems doubtful, however, that this equation can be applied to a neat liquid. For a few vanadyl triesters, coupling constants were calculated from quadrupole splittings of the NMR lines in nematic liquid crystals, taking $e^2qQ/h[VO(Oi\text{-}Pr)_3]$ as obtained directly from a powder spectrum for the determination of the ordering factor (150).

VI. CONCLUDING REMARKS

Among the quadrupolar transition metal nuclei, the vanadium nucleus may be considered the most favorable one for carrying out NMR experiments. This is due mainly to its rather small electric nuclear quadrupole moment (ca. $|0.05| \cdot 10^{-28}$ m^2), keeping quadrupolar relaxations rates sufficiently low to allow observation of well resolved spectra even for compounds of low point symmetry. At the same time NMR parameters arising from quadrupolar interactions (line widths in isotropic media, quadrupole splittings under anisotropic conditions) can be obtained in addition to the parameters commonly observed with spin 1/2 nuclei (chemical shifts and nuclear spin-spin coupling constants), providing a comprehensive set of data for different fields of application.

Due to the wide range of chemical shift values (caused by variations in the 2nd order paramagnetic deshielding contributions), spanning about 2500 ppm, the chemical shift is a sensitive probe to alterations in the first and also in the second coordination sphere of diamagnetic coordination compounds of vanadium in the formal oxidation states, -I, 0, +I, +III and +V. Applications go, however, beyond the identification of species, structural assignment and investigations of mechanistic aspects.

One of the areas of great promise encompasses methodological-theoretical statements on the basis of semi-quantitative analyses of ^{51}V NMR parameters, which will become more predominant as the NMR instrumentation is improved continuously and feasible vanadium complexes are increasingly prepared. The importance of vanadium NMR will thus shift towards a better understanding of the electronic interactions between vanadium and its ligand systems, providing results which may well apply to coordination compounds of other transition metals which are less accessible to NMR.

References

[1]V. Saraswati, J. Chem. Phys. Soc. Jpn. 23, 763 (1967).

[2]M. A. Habayeb and O. E. Hileman, Jr., Can. J. Chem. 58, 2115 (1980).

[3]W. J. Childs and L. S. Godman, Phys. Rev. 156, 64 (1967).

[4]K. Murakawa, J. Phys. Soc. Japan 21, 1466 (1966).

[5]R. A. Bennett and H. O. Hooper, J. Chem. Phys. 52, 5485 (1970).

[6]K. Murakawa, J. Phys. Soc. Japan 11, 422 (1956).

[7]J. O. Artman, Phys. Rev. 143, 541 (1966).

[8]E. Ertmer, U. Johann and G. Meisel, Phys. Lett. B85, 319 (1979).

[9]W. J. Childs, O. Poulsen, L. S. Godman and H. Crosswhite, Phys. Rev. A19, 168 (1979).

[10]O. Lutz, W. Messner, K. R. Mohn, and P. Kroneck, Z. Phys. A300, 111 (1981).

[11]H.-Ch. Bechthold and D. Rehder, J. Organometal. Chem., 206, 305 (1981); ibid. 233, 215 (1982).

[12]H. Ch. Bechthold, A. Keçeci, D. Rehder, H. Schmidt, and M. Siewing, Z. Naturforsch. B37, 631 (1982); A. Keçeci and D. Rehder, Z. Naturforsch. B36, 139 (1981).

[13]A. Yamasaki, Denki Tsuhin Daigaku Gakuho 27, 291 (1977).

[14]R. G. Kidd and R. J. Goodfellow, in NMR and the Periodic Table, R. K. Harris and B. E. Mann, Eds., Academic Press, New York, 1978, p. 195.

[15]R. G. Kidd, in Annual Reports on NMR Spectroscopy, G. A. Webb, Ed., Academic Press, New York 1978, Vol. 10A, p. 1.

[16]R. N. Pletnev, V. A. Gubanov, and A. A. Fotiev, YaMR v Oksidnykh Soyedineniyakh Vanadiya, Nauka, Moscow, 1979.

[17]A. Saika and C. P. Slichter, J. Chem. Phys. 22, 26 (1954).

[18]K. A. K. Ebraheem, G. A. Webb, and M. Witanowski, Org. Magn. Reson. 8, 317 (1976).

[19]D. Rehder, Z. Naturforsch. B32, 771 (1977).

[20]R. Talay and D. Rehder, Chem. Ber. 111, 1978 (1978).

[21]N. F. Ramsay, Phys. Rev. 78. 699 (1950).

[22]N. F. Ramsay, Phys. Rev. 86, 243 (1952).

[23]J. A. Pople, Discuss. Farad. Soc. 34, 7 (1962).

[24]J. A. Pople, J. Chem. Phys. 37, 53 (1962).

[25]T. Nakano, Bull. Chem. Soc. Japan 50, 661 (1977).

[26]H. Schmidt and D. Rehder, Trans. Met. Chem. 5, 214 (1980).

[27]J. S. Griffith and L. E. Orgel, Trans. Farad. Soc. 53, 601 (1957).

[28]J. S. Griffith, Ed., The Theory of Transition-Metal Ions, Cambridge University Press, New York/London, 1964, p. 284.

[29]N. Juranić, M. B. Celap, D. Vučelić, M. J. Malinar, and P. N. Radivojša, J. Magn. Reson. 35, 319 (1979).

[30]D. Rehder, J. Organometal. Chem. 37, 303 (1972).

[31]D. Rehder, W. L. Dorn, and J. Schmidt, Trans. Met. Chem. 1, 233 (1976).

[32]D. Rehder and J. Schmidt, J. Inorg. Nucl. Chem. 36, 333 (1974).

[33]D. Rehder, J. Magn. Reson. 25, 177 (1977).

[33a]R. Borowski, D. Rehder, and K. von Deuten, J. Organometal. Chem. 220, 45 (1981).

[34]R. Talay and D. Rehder, Z. Naturforsch. B36, 451 (1981).

[35]H. Baumgarten, H. Johannsen, and D. Rehder, Chem. Ber. 112, 2650 (1979).

[36]D. Rehder, J. Organometal. Chem. 137, C25 (1977).

[37]H.-Ch. Bechthold and D. Rehder, J. Organometal. Chem. 172, 331 (1979).

[38]W. R. W. Roose, D. Rehder, H. Lüders, and K. H. Theopold, J. Organometal. Chem. 157, 311 (1978).

[39]D. Rehder, J. Magn. Reson. 38, 419 (1980).

[40]D. Rehder, L. Dahlenburg, and I.

Müller, J. Organometal. Chem. 122, 53 (1976).
[41]I. Müller and D. Rehder, J. Organometal. Chem. 139, 293 (1977).
[42]D. Rehder and U. Puttfarcken, J. Organometal. Chem. 184, 343 (1980).
[43]D. Rehder, H.-Ch. Bechthold, and K. Paulsen, J. Magn. Reson. 40, 305 (1980).
[44]D. Rehder and J. Schmidt, Trans. Met. Chem. 2, 41 (1977).
[45]D. Rehder, W. L. Dorn, and J. Schmidt, Trans. Met. Chem. 1, 74 (1976).
[46]U. Puttfarcken and D. Rehder, J. Organometal. Chem. 185, 219 (1980); D. Rehder and U. Puttfarcken, Z. Naturforsch. B37, 348 (1982).

[47]F. Näumann and D. Rehder, J. Organometal. Chem. 204, 411 (1981).
[48]M. Herberhold, and H. Trampisch, Z. Naturforsch. B37, 614 (1982).
[49]U. Puttfarcken and D. Rehder, J. Organometal. Chem. 157, 321 (1978).
[50]J. Schiemann, E. Weiss, F. Näumann, and D. Rehder, J. Organometal. Chem. 232, 219 (1982).
[51]K. von Deuten, D. Rehder, and W. Roose, J. Organometal. Chem. 214, 71 (1981).
[52]U. Mollers, Dissertation, Hamburg, 1979.
[53]O. W. Howarth, private communication.
[54]R. L. Martin and A. H. White, Nature 223, 394 (1969).
[55]A. Yamasaki, F. Yayima, and S. Fujiwara, Inorg. Chim. Acta 2, 39 (1968).
[56]A. Yamasaki, F. Yayima, and S. Fujiwara, J. Magn. Reson. 1, 203 (1969).
[57]G. G. Mather, A. Pidcock, and G. J. M. Rapsey, J. Chem. Soc. Dalton Trans., 2095 (1973).
[58]P. B. Hitchcock, B. Jacobson, and A. Pidcock, J. Chem. Soc. Dalton Trans., 2038 (1977).
[59]J. MacLeod, L. Manojlović-Muir, D. Millington, K. W. Muir, D. W. A. Sharp, and R. Walker, J. Organometal. Chem. 97, C7 (1975).
[60]P. S. Braterman, R. J. Cross, L. Manojlović-Muir, K. W. Muir, and G. B. Young, J. Organometal. Chem. 84, C40 (1975).
[61]G. J. Palenic, M. Mathew, W. L. Steffen, and G. Beran, J. Am. Chem. Soc. 97, 1059 (1975).
[62]W. L. Steffen and G. Palenic, Inorg. Chem. 15, 2432 (1976).
[63]P. B. Hitchcock, B. Jacobson, and A. Pidcock, J. Chem. Soc. Dalton Trans., 2038 (1977).
[64]R. Lenck, Dissertation Hamburg (1973).
[65]K. Paulsen, D. Rehder, and D. Thoennes, Z. Naturforsch. A33, 834 (1978).
[66]J. V. Hatton, Y. Saito, and W. G. Schneider, Can. J. Chem. 43, 47 (1965).
[67]J. A. S. Howell and K. C. Moss, J. Chem. Soc. A, 270 (1971).
[68]Yu. A. Buslaev, V. D. Kopanev, A. A. Konovalova, S. V. Bainova, and V. P. Tarasov, Dokl. Akad. Nauk SSR 243, 1175 (1978); Dokl. Chem. 243, 583 (1978).
[69]S. E. O'Donnell and M. T. Pope, J. Chem. Soc. Dalton Trans., 2290 (1976).
[70]O. W. Howarth and J. R. Hunt, J. Chem. Soc. Dalton Trans., 1388 (1979); E. Heath and O. W. Howarth, ibid. 1105 (1981).
[71]C. M. Flynn, Jr., M. T. Pope, and S. O'Donnell, Inorg. Chem. 13, 831 (1974).
[72]O. W. Howarth and R. E. Richards, J. Chem. Soc., 864 (1965).
[73]L. P. Kazanskii and V. I. Spitsyn, Dokl. Akad. Nauk. SSR 223, 381 (1975); Dokl. Phys. Chem. 223, 721 (1975).
[74]Yu. A. Buslaev, V. P. Tarasov, S. M. Sinitsyna, V. G. Khelebodarov, and V. D. Kopanev, Koord. Khim. 5, 189 (1979).
[75]A. Lachowicz and K.-H. Thiele, Z. Anorg. Allgem. Chem. 434, 271 (1977).
[76]K. Witke, A. Lachowicz, W. Bruser, and D. Zeigan, Z. Anorg. Allgem. Chem. 465, 193 (1980).
[77]A. G. Swallow, F. R. Ahmed, and W. H. Barnes, Acta Cryst. 21, 397 (1966).
[78]O. Lutz, W. Nepple, and A. Nolle,

Z. Naturforsch. A31, 1046 (1976).
[79]O. W. Howarth and M. Jarrold, J. Chem. Soc. Dalton Trans., 503 (1978).
[80]W. G. Klemperer and W. Shum, J. Am. Chem. Soc. 99, 3544 (1977).
[81]L. P. Kazanskii, M. A. Fedotov, M. N. Ptushkina, and V. I. Spitsyn, Dokl. Akad. Nauk. SSR 240, 117 (1978); Dokl. Chem. 240, 422 (1978).
[82]R. I. Maksimovskaya, M. A. Fedotov, V. M. Mastikhin, L. I. Kuznetsova, and K. I. Matveev, Dokl. Akad. Nauk. SSR 240, 117 (1978); Dokl. Chem. Proc. Acad. Sci. 240, 422 (1978).
[83]S. P. Harmalker, M. A. Leparulo, and M. T. Pope, XXI. ICCC, Toulouse 1980, and M. T. Pope, private communication.
[83a]K. Ihmels and D. Rehder, J. Organometal. Chem. 218, C54 (1981).
[84]P. E. Garrou, Chem. Rev. 81, 229 (1981).
[85]T. G. Appleton, U. A. Bennett, and I. B. Tomkins, J. Chem. Soc. Dalton Trans., 439 (1976).
[86]S. Hietkamp, D. J. Stufkens, and K. Vrieze, J. Organometal. Chem. 169, 107 (1979).
[87]S. O. Grim, W. L. Briggs, R. C. Barth, C. A. Tolman, and J. P. Jessen, Inorg. Chem. 13, 1095 (1974).
[88]R. Freeman, G. R. Murrary, and R. E. Richards, Proc. Roy. Soc. A242, 455 (1957).
[89]J. F. Nixon and A. Pidcock, Adv. Nucl. Magn. Reson. 2, 345 (1969).
[90]P. S. Pregosin and R. W. Kunz, in NMR - Basic Principles and Progress, P. Diehl, E. Fluck, and R. Kosfeld, Eds., Springer Verlag, Berlin, 1979, Vol 16, p. 1.
[91]G. M. Whitesides and H. L. Mitchell, J. Am. Chem. Soc. 91, 2245 (1969).
[92]U. Franke and E. Weiss, J. Organometal. Chem.153, 39 (1978).
[93]U. Franke, Dissertation Hamburg 1978.
[94]G. M. Bodner and L. J. Todd, Inorg. Chem. 13, 1335 (1974).
[95]H. S. Gutowsky, D.W. McCall, and C. P. Slichter, J. Chem. Phys. 21, 279 (1953).
[96]P. C. Lauterbur and R. B. King, J. Am. Chem. Soc. 87, 3266 (1966).
[96a]W. A. Nugent and R. L. Harlow, Chem. Commun., 342 (1979).
[97]E. M. Hyde, J. D. Kennedy, B. L. Shaw, and W. McFarlane, J. Chem. Soc. Dalton Trans., 1571 (1977).
[98]S. O. Grim and D. A. Wheatland, Inorg. Chem. 8, 1716 (1969).
[99]W. McFarlane, J. Chem. Soc. Dalton Trans., 324 (1974).
[100]H. C. E. McFarlane, W. McFarlane, and R. J. Wood, Bull. Soc. Chim. 85, 864 (1976).
[101]J. D. Kennedy, W. McFarlane, R. J. Puddephatt, and P. J. Thompson J. Chem. Soc. Dalton Trans., 874 (1976).
[102]R. Meij, D. J. Stufkens, K. Vrieze, E. Roosendaal, and H. Schenk, J. Organometal. Chem. 155, 323 (1978).
[103]J. Chatt, R. Mason, and D. W. Meek, J. Am. Chem. Soc. 97, 3826 (1975).
[104]D. S. Milbrath, J. G. Verkade, and R. J. Clark, Inorg. Nucl. Chem. Lett. 12, 921 (1976).
[105]S. O. Grim, R. R. McAllister, and R. M. Singer, Chem. Comm., 38 (1969).
[106]C. E. Jones and K. J. Coskran, Inorg. Chem. 10, 55 (1971).
[107]J. Schmidt, Z. Naturforsch. B27, 600 (1972).
[108]J. M. Bancroft, H. C. Clark, R. G. Kidd, A. T. Rake, and H. G. Spinney, Inorg. Chem. 12, 728 (1973).
[109]D. E. O'Reilley and G. E. Schacher, J. Chem. Phys. 39, 1768 (1968).
[110]R. T. Obermeyer and E. P. Jones, J. Chem. Phys. 58, 1677 (1973).
[111]K. T. Gillen and J. H. Noggle, J. Chem. Phys. 53, 801 (1970).
[112]A. D. Buckingham and K. A. McLauchlan, in Progress in NMR Spectroscopy, J. W. Emsley, J. Feeney, and L. H. Sutcliffe, Eds., Pergamon Press, Oxford, 1967, Vol. 2, pp. 63-73.
[113]D. Lindman and S. Forsén, in NMR - Basic Principles and Progress, P. Diehl, E. Fluck, and R. Kosfeld, Eds., Springer Verlag, Berlin, 1976, Vol. 16, pp. 233-238.
[114]D. Rehder, K. Paulsen, and H.

Lechert, Z. Naturforsch. A33, 1597 (1978).
[115]P. W. France, J. Magn. Reson. 34, 585 (1979); ibid. 40, 311 (1980).
[116]S. D. Gomostansky and C. V. Stager, J. Chem. Phys. 46, 4959 (1967).
[116a]J. L. Ragle, J. Chem. Phys. 35, 753 (1961).
[117]L. Facchini, C. Sanchez, J. Livage and A. P. Legrand, Joint ISMAR-AMPERE Conference, Delft 1980.
[118]R. N. Pletnev, A. A. Sidorov, V. A. Peveljaev, and Yu. M. Beljakov, Dokl. Akad. Nauk. SSR 245, 144 (1979).
[119]R. N. Pletnev, A. A. Fotiev, L. V. Zolotuchina, and V. K. Kaputskin, Dokl. Akad. Nauk. SSR 241, 873 (1978).
[120]A. G. Petrov, R. N. Pletnev, L. V. Zolotukhina, and V. A. Gubanov, Izv. Akad. Nauk SSR, Neorg. Mater. 16, 678 (1980).
[121]L. V. Zolotukhina, R. N. Pletnev, A. A. Fotiev, and V. K. Kaputskin, Zh. Neorg. Khim. 23, 27 (1978); Russ. J. Inorg. Chem. 23, 15 (1978).
[122]K. Narita, J. Umeda, and H. Kusumoto, J. Chem. Phys. 44, 2719 (1966).
[123]S. Tagagi, Y. Kitaoka, H. Yasuoka, T. Ohtani, K. Kosuge, and S. Kachi, J. Phys. Soc. Jpn. 49, 521 (1980).
[124]Y. Ueda, K. Kosuge, and S. Kachi, J. Solid State Chem. 31, 171 (1980).
[125]K. Maruyama and H. Nagasawa, J. Phys. Soc. Jpn. 48, 2159 (1980).
[126]R. N. Pletnev, W. N. Lisson, Yu. M. Beljukov, and J. J. Miller, Inst. Khim. (Akad. Nauk. SSSR Ural'skij Filial) Trudy. Sverdlovsk 32, 32 (1975).
[127]J. E. Baugher, P. C. Taylor, T. Oja, and P. J. Bray, J. Chem. Phys. 50, 4914 (1969).
[128]R. N. Pletnev, V. A. Gubanov, and A. K. Chirkov, Zh. Strukt. Khim. 17, 938 (1976); J. Struct. Chem. 17, 805 (1976).
[129]R. N. Pletnev, V. V. Gorshkov, and A. A. Ivakin, Zh. Neorg. Khim. 21, 331 (1976); Russ. J. Inorg. Chem. 21, 178 (1976).
[130]S. D. Gomostansky and C. W. Stager, J. Chem. Phys. 48, 1416 (1968).
[131]S. L. Segel and R. B. Creel, Can. J. Phys. 48, 2673 (1970).
[132]V. A. Gubanov, N. I. Lazukova, and R. N. Pletnev, Zh. Neorg. Khim. 23, 655 (1978); Russ. J. Inorg. Chem. 23, 362 (1978).
[133]S. I. Andronenko, L. V. Dmitrieva, N. G. Molodchenko, V. V. Moskalev, and Z. N. Zonn, Fiz. Tverd. Tela 21, 914 (1979); Sov. Phys. Solid State 21, 535 (1979).
[134]V. A. Ioffe, L. V. Dmitrieva, A. P. Vereshchagina, Z. N. Zonn, and S. I. Andronenko, Fiz. Tverd. Tela 19, 1204 (1977); Sov. Phys. Solid State 19, 704 (1977).
[135]R. N. Pletnev, N. I. Lazukova, and V. A. Gubanov, Zh. Fiz. Khim. 51, 2359 (1977); Russ. J. Phys. Chem. 51, 1382 (1977).
[136]V. A. Gubanov, R. N. Pletnev, V. N. Lisson, and A. K. Chirkov, Spectr. Lett. 10, 527 (1977).
[137]A. A. Sidorov, V. N. Lisson, R. N. Pletnev, and W. A. Gubanov, Fiz. Tverd. Tela 17, 2427 (1975).
[138]G. V. Basuev, R. N. Pletnev, W. K. Slebuchin, V. N. Lisson, and G. P. Shveykin, Izvest. Neorg. Materialy. 14, 711 (1978).
[139]R. N. Pletnev, A. A. Sidorov, V. N. Lisson, and A. K. Chirkov, Dokl. Akad. Nauk. SSR 236, 1159 (1977).
[140]R. N. Pletnev, V. N. Lisson, G. V. Basuev, and G. P. Shveikin, Radiospektroskopiya (Perm), 28 (1978).
[141]B. Bleaney and M. R. Wells, Proc. Roy. Soc. (London) A370, 131 (1980).
[142]B. Bleaney and M. R. Wells, Joint ISMAR-AMPERE Conference, Belft 1980.
[143]B. Bleaney, A. C. de Oliveira, and M. R. Wells, Joint ISMAR-AMPERE Conference, Delft 1980.
[144]M. Bose, S. Ganguli, and M. Bhattacharya, Phys. Rev. B19, 5535 (1979).
[145]B. Bleaney, F. N. H. Robinson, and M. R. Wells, Proc. Roy. Soc.

A362, 179 (1978).
[146]R. B. Creel and E. von Meerwall, J. Chem. Phys. 73, 1538 (1980).
[147]A. C. Gossard, Phys. Rev. 149, 246 (1966).
[147a]A. V. Skripov, A. P. Stepanov, V. A. Marchenko, V. M. Pan, and A. D. Shevchenko, Zh. Eksp. Teor. Fiz. 77, 2313 (1979); Sov. Phys. 50, 1113 (1980).
[148]P. K. Burkert, M. F. Eckel, and H.-P. Fritz, Magn. Reson. Related Phenomena, Proc. Congr. AMPERE, 17th (1972), p. 263.
[149]A. Allerhand, J. Chem. Phys. 52, 2162 (1970).
[150]K. Paulsen and D. Rehder, Z. Naturforsch. A37, 139 (1982).
[151]A. Abragam, The Principles of Nuclear Magnetism, Oxford University Press, Oxford, 1961, p. 348.
[152]P. A. Casabella, J. Chem. Phys. 40, 149 (1964).